

UNIVERSIDADE ESTADUAL PAULISTA JULIO DE MESQUITA FILHO
FACULDADE DE ENGENHARIA
CAMPUS DE ILHA SOLTEIRA

ALINE PETEAN PINA

**SINGULAR VALUE ANALYSES OF VOLTAGE STABILITY ON POWER SYSTEM
CONSIDERING WIND GENERATION VARIABILITY**

Ilha Solteira

2015

ALINE PETEAN PINA

**SINGULAR VALUE ANALYSES OF VOLTAGE STABILITY ON POWER SYSTEM
CONSIDERING WIND GENERATION VARIABILITY**

Tese apresentada à Faculdade de Engenharia do Câmpus de Ilha Solteira - UNESP como parte dos requisitos para obtenção do título de Doutor em Engenharia Elétrica. Especialidade: Automação.

Prof. Dr. Percival Bueno de Araujo

Orientador

Prof. Dr. Bala Venkatesh

Co-orientador

Ilha Solteira

2014

FICHA CATALOGRÁFICA

Desenvolvido pelo Serviço Técnico de Biblioteca e Documentação

- P645s Pina, Aline Petean .
Singular value analyses of voltage stability on power system considering wind generation variability / Aline Petean Pina. -- Ilha Solteira: [s.n.], 2014 75 f.
- Tese (doutorado) - Universidade Estadual Paulista. Faculdade de Engenharia de Ilha Solteira. Área de conhecimento: Automação, 2014
- Orientador: Percival Bueno De Araujo
Co-orientador: Bala Venkatesh
Inclui bibliografia
1. Sistema elétrico. 2. Estabilidade de tensão. 3. Energia eólica.
4. Mínimos valores singulares. 5. Incerteza. 6. Variação do vento.

CERTIFICADO DE APROVAÇÃO

TÍTULO: Singular Value Analyses of Voltage Stability on Power System Considering Wind Generation Variability

AUTORA: ALINE PETEAN PINA

ORIENTADOR: Prof. Dr. PERCIVAL BUENO DE ARAUJO

CO-ORIENTADOR: Prof. Dr. BALA VENKATESH

Aprovada como parte das exigências para obtenção do Título de DOUTOR EM ENGENHARIA ELÉTRICA, Área: AUTOMAÇÃO, pela Comissão Examinadora:



Prof. Dr. PERCIVAL BUENO DE ARAUJO

Departamento de Engenharia Elétrica / Faculdade de Engenharia de Ilha Solteira



Prof. Dr. DILSON AMANCIO ALVES

Departamento de Engenharia Elétrica / Faculdade de Engenharia de Ilha Solteira



Prof. Dr. FÁBIO BERTEQUINI LEÃO

Departamento de Engenharia Elétrica / Faculdade de Engenharia de Ilha Solteira



Prof. Dr. GIDEON VILLAR LEANDRO

Departamento de Engenharia Elétrica / Universidade Federal do Paraná



Prof. Dr. MARCOS AMORIELLES FURINI

Coodenação Da Área de Indústria / Instituto Federal de São Paulo - Ifsp

Data da realização: 05 de dezembro de 2014.

I dedicate this work to my parents, Lázaro and Magda.

ACKNOWLEDGEMENTS

I would like to thank Professor Percival Bueno de Araujo for his patience, continuous advice and mentorship, during several years of working together. His comments have been inestimable.

I also thank Professor Bala Venkatesh for his wise counsel. This thesis was prepared with his efforts and expertise that would have been impossible to reach without his support and leadership.

My sincere thanks are also to Professors Anna Diva Plasencia Lotufo, Antônio Padilha Feltrin, Dilson Amâncio Alves, Fábio Bertequini Leão and Laurence Duarte Colvara.

I am grateful to the UNESP University, which provided me with working environment to pursue my goals. My special thanks go to Dr. Augusto Cesar Rueda Medina for assistance and support.

I also thank the Ryerson University, Centre for Urban Energy (CUE), for providing an excellent working environment. My special thanks go to Dr. Chandrabhanu Opathella for a working environment which permitted me to pursue my goals.

I thank all the members of CUE for their support and for helping me learning English and all members of GAESEE for fellowship. Special thanks to my friend Naryanne Rodrigues Peraro.

Generous funding was provided by the CAPES and CNPq.

I thank my whole family; they were always encouraging me and guiding me. My special thanks to my sister Ticiania and my brother-in-law Aurasil.

"They can burn books, but do not burn ideas; the flames of the fires stimulate rather than extinguish them. Moreover, the ideas are in the air, and there is no quite high Pyrenees to stop them; and when they are great and generous, find thousands of willing hearts to crave it. "

Allan Kardec

RESUMO

Os sistemas de transmissão em todo o mundo, que foram projetados e construídos para operar, predominantemente, com geração síncrona convencional, como a geração hídrica. Entretanto, agora se faz necessária a integração de energia renovável, tais como a energia eólica e energia solar. Estes geradores de energias renováveis estão localizados em locais ricos em recursos, causando uma injeções de potência em sistemas de transmissão, submetendo-os a indevidos esforços e obrigando-os a operar em novos pontos de operação. Em muitos sistemas de transmissão, a capacidade de integração se aproximou do limite, sendo necessárias atualizações para acomodar uma maior penetração de geração eólica. Os exemplos podem ser vistas na Alemanha, Ontario (Canadá) e Texas. Nestas situações, onde as capacidades do sistema de transmissão estão próximas do limite de operação, é importante para avaliar a estabilidade de tensão, considerando (a) a geração eólica e (b) possível efeito da incerteza na previsão. Neste trabalho, é proposta uma abordagem sistemática para estabilidade de tensão. Com a utilização de um algoritmo de fluxo de potência ótimo e da construção da matriz hessiana, será determinada a relação entre as mudanças nos valores mínimos singulares do sistema Jacobiano e as mudanças na injeção de potência no barramento em tempo real. Esta relação é usada para examinar o efeito da incerteza da previsão de energia eólica na estabilidade de tensão. O método proposto é usado para estudar os efeitos da incerteza sobre a estabilidade de tensão dos sistemas 6-barras, 57-barras e 118-barras do IEEE; do Sistema Sul Brasileiro reduzido e também foi usado um sistema real 600 barras. Os resultados são detalhados nesta tese.

Palavras-chave: Fluxo de potência. Estabilidade do sistema elétrico. Decomposição em valores singulares. Incerteza. Variação do vento.

ABSTRACT

Transmission Systems worldwide, that were designed and built to operate with predominantly conventional synchronous generation, are advancing to integrate large amounts of renewable energy generators. These renewable generators are sited at resource-rich locations, causing a geographical shift in power injections into transmission systems, subjecting them to undue stress and making them operate in new states. In many transmission systems, capacities to integrate wind resource are exhausted or are being upgraded to accommodate higher wind generation penetration. Examples may be seen in Germany, Ontario (Canada) and Texas. In these situations, where transmission system capacities have been reached, it is important to assess voltage stability by considering (a) wind generation and (b) possible effect of uncertainty in forecast. In this work, a systematic approach of studying voltage stability is proposed. Using an optimal power flow algorithm, the Hessianmatrix of power balance equations is determined that relates changes in minimum singular values of system Jacobian to changes in bus-wise real power injections. This relationship is used to examine effect of uncertainty of wind power forecast on voltage stability. The proposed method is used to study the effects of uncertainty on system voltage stability of 6-bus, 57-bus and 118-bus IEEE and 45-bus South Brazilian test systems, for the real analyses is used 600-bus and results are reported. Considering the simplification of computation, the proposed method has a clear advantage compared to the conventional Jacobian technique using repeated OPF solutions.

Keywords: Power flow. Voltage stability. Singular value decomposition. Wind variation.

LIST OF FIGURES

Figure 1 - World Total Installed Capacity.....	20
Figure 2 - World Total Installed Capacity.....	21
Figure 3 - World Market Growth Rates	21
Figure 4 - New Installed Capacity 2013.....	22
Figure 5 - Total Installed Capacity 2013.....	23
Figure 6 - Annual Installed Capacity for Region 2005-2013	24
Figure 7 - Market Forecast for 2014-2018	27
Figure 8 - Annual Market Forecast by Region for 2013-2018.....	27
Figure 9 - Cumulative Market Forecast by Region for 2013-2018.....	28
Figure 10 - Wind energy in Blue map of IEA/ GWEC	30
Figure 11 - Global electricity mix by 2050 in the 2DS and hiRen scenario	31
Figure 12 - Regional production of wind electricity in the 2DS and hiRen.....	32
Figure 13 - Installed capacity in Brazil	34
Figure 14 - Normal distribution of wind power output forecast	40
Figure 15 - The 6-Bus System.....	43
Figure 16 - Minimum singular value versus $\Delta\Sigma$ for 6-bus system.....	45
Figure 17 - The 57-Bus System.....	45
Figure 18 - MSV versus $\Delta\Sigma$ for 57- bus system.....	47
Figure 19 - The IEEE 118-Bus System	47
Figure 20 - MSV versus $\Delta\Sigma$ for 118 bus system	49
Figure 21 - Southern Brazilian Reduced System	50
Figure 22 - MSV versus $\Delta\Sigma$ for the Southern Brazilian Reduced System	52
Figure 23 - MSV versus $\Delta\Sigma$ for 581- Bus System.....	53

LIST OF TABLES

Table 2 - Minimum Singular Values of the 6-Bus Test System.....	44
Table 3 - Variation of Smallest $\Delta\Sigma$ of the 57-Bus Test System	46
Table 4 - Smallest MSV of 57-Bus Test System.....	46
Table 5 - Variation of Smallest $\Delta\Sigma$ of 118-Bus Test System	48
Table 6 - Smallest MSV of 118 Bus Test System	48
Table 7 - Variation of Smallest $\Delta\Sigma$ of the Southern Brazilian Reduced System	51
Table 8 - Smallest MSV of the Southern Brazilian Reduced System	51
Table 9 - Variation of Smallest $\Delta\Sigma$ of 581- Bus System.....	52
Table 10 - Smallest MSV of 581- Bus System.....	53

LIST OF SYMBOLS

The main symbols used in this thesis are listed below for quick reference. Other symbols are defined as needed throughout the text.

V, δ	Bus voltage magnitude and phase angle
P, Q	Bus real and reactive power injections
H_δ	Hessian matrix
$J_{P\delta}$	Reduced Jacobian matrix
J_1, J_2, J_3, J_4	Components of the Jacobian matrix
PD, QD	Bus real and reactive power demand
PG, QG	Bus real and reactive power generation
\hat{P}_W	Mean wind power output
SU, SV	Left and right singular matrices
T	Matrix transposed
Σ	Diagonal matrix comprising singular values
ΔV	Vector of change of bus voltage magnitudes
$\Delta \delta$	Vector of change of bus voltage angles
ΔP	Vector of change of bus real power injections
ΔQ	Vector of change of bus reactive power injections
$\Delta \Sigma$	Variance effect in minimum singular value
MSV	Minimum Singular Value
I	Index for bus number
NB	Number of buses
PDF	Probability Density Function

TABLE OF CONTENTS

1	INTRODUCTION	11
1.1	LITERATURE SURVEY OF VOLTAGE STABILITY STUDIES	12
1.2	EFFECT OF WIND ENERGY ON VOLTAGE STABILITY	15
1.3	MOTIVATION OF THIS THESIS	16
1.4	OBJECTIVES	17
1.5	ORGANIZATION OF THIS THESIS	17
1.6	CHAPTER SUMMARY	18
2	PANORAMA OF WIND POWER IN BRAZIL AND THE WORLD.....	19
2.1	WORLD	19
2.1.1	Current Capacity.....	20
2.1.2	Capacity factor	24
2.1.3	Projections of the future market for wind energy.....	25
<i>2.1.3.1</i>	<i>Market Forecast for 2014-2018</i>	<i>25</i>
<i>2.1.3.2</i>	<i>Long-Term Market Forecast.....</i>	<i>29</i>
2.2	BRAZIL.....	32
2.3	CHAPTER SUMMARY	35
3	PROPOSED METHOD OF ANALYSES OF VOLTAGE STABILITY.....	36
3.1	VOLTAGE STABILITY AND MINIMUM SINGULAR VALUE OF SYSTEM JACOBIAN	36
3.1.1	Minimum Singular Value Methods	37
3.2	EFFECT OF WIND POWER UNCERTAINTY ON VOLTAGE STABILITY	39
3.3	CHAPTER SUMMARY	41
4	TEST AND RESULTS.....	42
4.1	DESCRIPTION OF TEST SYSTEMS	42
4.1.1	Ward and Hale 6-Bus System.....	43
4.1.2	IEEE 57-Bus System	45
4.1.3	IEEE 118-Bus System	47
4.1.4	Southern Brazilian Reduced System	49
4.1.5	An Actual System	52
4.2	CHAPTER SUMMARY	54
5	CONCLUSION.....	55
5.1	RESEARCH CONTRIBUTIONS	55
5.2	FUTURE WORK	55
	REFERENCES	57
	APPENDIX A – Data of systems.....	62
	APPENDIX B - Introduction to Taylor's theorem for multivariable functions...	72

1 INTRODUCTION

The increasing demand for energy cleared the way for inclusion of new sources of renewable energy in power systems, making them more complex. In this context, wind energy supply has experienced phenomenal growth in the last 20 years, particularly in the United States, Europe, China and India. Preliminary estimates suggest worldwide wind energy installations were 34-35 GW in 2013, "a substantial dropoff" from a record-setting 2012, according to Global Wind Energy Council (GWEC). This year promises to be significantly better (though perhaps not quite so good as 2012), with expectations of stabilization and growth in both the U.S. and China, and continued strength building in some emerging markets, like Brazil, where the total installed capacity of all wind farms is 3,331 MW according to Câmara de Comercialização de Energia Elétrica (CCEE). Moreover, GWEC's initial expectations for 2014 are for 45-48 GW, and with some upside.

When the power systems are being integrated with more renewable energy sources, active and reactive power sources are replaced with active power only sources. Furthermore, power system active power generation becomes more uncertain and geographically spread all over the system. Because of this reason, with the current trend of renewables, systems operate very close to their limits. Consequently, power systems become most vulnerable to contingencies. This situation contributes to overload condition in the transmission lines, disrespect the voltage limits and may cause instability problems; therefore, safety problem with the power system. Thus, some disturbances may lead the system to lose synchronism and even a possible blackout.

Faced with the significant increase of energy sources, currently, power systems integrating large amounts of wind power have become intricate systems in diverse aspects of their operation and control (ELA et al., 2009; RAVE, 2013). Power system operators confront challenges associated to different operation characteristics of each energy source, e.g., voltage stability arising from many factors such as thermal limitations of lines, generator controls, etc. In an optimally scheduled power system, once these limits are reached, it becomes more vulnerable to voltage collapse and system instability. Because of this reason, power systems need some changes to improve deteriorating voltage stability margins (BEN-KILANI; ELLEUCH, 2013).

1.1 LITERATURE SURVEY OF VOLTAGE STABILITY STUDIES

This work addresses the problem of voltage stability with uncertainty in wind energy sources. This Section surveys the literature to show the main references that make use of concepts and methods associated with this mode of study.

Voltage stability is a well-researched area in power system analysis. Voltage stability can be approached from two points of view: static and dynamic. The dynamic character requires treatment as a phenomenon that can be modeled with a set of nonlinear differential equations (VU et al., 1995). This is a complex and sophisticated analysis, especially when dealing with large systems. An easier but equally important form of the voltage stability study refers to the observation of the behavior of the node voltages, considering the gradual increase of the system load profile, i.e., the qualitative analysis of the operating point. In this case, the analysis can be treated as a linear problem.

In a noteworthy publication, Van Cutsem (2000) addressed topics such as Bifurcations, load dynamics, nonlinear systems, security analysis. Significant comparisons of various methods to study the voltage stability are established.

Many system-oriented approaches and long-term voltage-stability methods are based on static models because of the high dimensionality and complexity of stability problems. For this reason, control-actions, time-range, quasi-steady-state time-domain simulations are used to simplify matters (VAN CUTSEM, 1998). The results of such studies can also be used for screening purposes to identify critical cases that require a more detailed or dynamic analysis (MORISON et al., 1993).

Sauer and Pai (1990) presented a methodology based on the model of power flow using Newton's method. Appropriate versions to resolve the question of stability based on Newton's method employ the method of continuation, i.e., are iterative search procedures of the "tip of the nose" (extreme point) of PV (CHEN et al., 2002). Many other publications use the same technique (ZAMBRONI, 2000; CHEN et al., 2002; ALVES et al., 2003).

Inferences about the system are based on analysis of the behavior of the equilibrium point, more specifically, from the analysis of the Jacobian matrix based on power-balance equations, constituting an incremental power flow problem formulated via Newton-Raphson (ARYA; CHOUBE; SHRIVASTAVA, 2008; JIA, 2000; NAN et al., 2000; SINHA; HAZARIKA, 2000; TIRANUCHIT; THOMAS, 1988). In this case, Jacobian matrix is calculated at the operating point.

Thus, from the analysis of the Jacobian matrix, stability is examined. This analysis can be performed, for example, using eigenvalue decomposition and eigenvectors of the Jacobian matrix (PETEAN-PINA; ARAUJO, 2010; TIRANUCHIT; THOMAS 1988), tangent vector (ZAMBRONI, 2000), among other techniques. The system behavior for small disturbances may be analyzed using the eigenvalues of the Jacobian matrix. If all eigenvalues own positive real part, it is possible to conclude that the system is stable for small perturbations. However, the instability is characterized by having at least one eigenvalue with a negative real part (TIRANUCHIT; THOMAS 1988). The limit point happens when the Jacobian matrix becomes singular, i.e., the determinant of the Jacobian becomes null. Most of the publications addressed this issue in the same way. In Smith et al., (2007), the dynamic voltage collapse indicator DVCI is implemented using maximum loadability index (MLI). Even for a stable system, system operator would like to operate the power system maintaining an appropriate margin to the voltage collapse points. Ultimately, the power system should be able to maintain its stability even at an expected contingency. If the system is close to the voltage collapse point, reactive power compensation techniques are used for correcting the voltage profile. Traditionally, synchronous generators, capacitor banks and FACTS devices are used for the reactive power compensations.

Ajjarapu and Christy (1992) proposed the calculation of power flow using the continuation method, called UWPFLOW, from the base case of loading to look for the limit of the voltage stability. This reference demonstrates the ability of the continuation method in solving problems in power systems. The method of continuation employs a predictor-corrector search for the extreme point of the P-V curve. Canizares and Alvarado (1996) present new results based on the use of the method UWPFLOW of Ajjarapu and Christy (1992). Chiang (2002) proposed another computational program designated CPFLOW (Continuation Power Flow), to improve the UWPFLOW performance of the software. A new index was developed for the analysis of voltage stability based on the concept of center manifolds and normal forms (GUCKENHEIMER; HOLMES, 1997). The CPFLOW generates P-P, Q-Q and P-V-V curves.

Vournas(1995) presents a voltage stability index (VSI) and a voltage controllability index (VCI), related to the eigenvalues of $m \times m$ matrices in a multimachine power system. System loads had an arbitrary voltage sensitivity described by generalized voltage exponents. The approach followed in the paper provides two other important indices, the algebraic equation Jacobian determinant, and the VCI.

De Souza et al. (1997) proposed a method using tangent vector to define an indication at any operating condition of the critical area at the collapse point, and a voltage stability index

is defined based on the identification of this critical area. Also, a predictor-corrector methodology based on this index and the continuation method was proposed for computations of voltage collapse points.

Ideally, if the system voltages are above the collapse voltage, it is a stable system. Traditionally a non-zero minimum singular value of system Jacobian indicates that the system is voltage stable (LOF et al., 1992). While, the minimum singular value by itself does not quantify the distance to voltage collapse; whereas, change in its value is an indication of change in system voltage stability.

The Tellegen's theorem and adjoint networks are used to derive a new, local voltage-stability index in Smon et al. (2006). It requires the voltage and current phasors measurements only to evaluate the system's voltage stability at a bus, which makes it very appealing for phasor measurement units (PMU) -based online monitoring and protection schemes.

Along with this simple index, in literature, it is noted that several researchers have been looking for voltage collapse indices. The method in Verbic and Gubina(2003, 2004), applies phasors calculated at the relaying point to compute the S Difference Criterion (SDC) value. Then, when the SDC drops below 0.2, the relay sets off as a mitigation procedure.

Venkatesh et al. (2007), presents the dynamic voltage collapse indicator DVCI using maximum loadability index (MLI). Even for a stable system, the system operator would like to operate the power system maintaining an appropriate margin to voltage collapse. Further, the power system is expected to be voltage stable after an N-1 contingency. In weak systems, reactive power compensation techniques are used to improve system margin to voltage collapse. Traditionally, synchronous generators, capacitor banks and FACTS devices work for the reactive power compensations.

InLeonardi and Ajjarapu_(2011), system wide reactive power reserve is related to voltage stability margin. This relationship is established using a statistical multi-regression technique and offline data. Once the statistical relationship is established, it can be used as an online tool to examine voltage stability margin at any system loading level.

1.2 EFFECT OF WIND ENERGY ON VOLTAGE STABILITY

The integration of new renewable energy plants, as wind plants, into a well-established power system may be challenging as their power output cannot be controlled in the same manner as traditional power plants, such as thermal or hydro-based generators. Further, the power output by wind plants, like all weather-driven renewable sources, can be characterized as being variable and uncertain, which may detrimentally affect the operation of the system (SMITH et al., 2009; SMITH et al., 2007). By the way, the power from wind plants tends to evidence diurnal and seasonal standard. The timing and severity of the standard may amplify the challenge of integrating the wind plants if, for example, an overflow of wind power usually occurs during periods of low demand. Many factors, like the penetration level and geographic dispersal of the wind plants within the power system, influence the characteristics of variability, uncertainty and timing and strength of the standard of the wind power (SMITH et al., 2007). Understanding the characteristics of the wind power in a system is an important step in developing efficient and cost-effective operational and technological wind plant integration-enabling solutions (LOUIE, 2010).

For this reason, with the current trend of renewable energy sources, there is a renewed research interest on voltage stability. In a recent research study (BEN-KILANI; ELLEUCH, 2013) voltage stability with wind power integration is discussed. A modified Jacobian matrix is created with sub matrices based on bus types. In this bus classification, buses with synchronous generators, doubly-fed induction generators, constant speed induction generators and loads represent different sub matrices. Then, the minimum singular value technique is used for investigating voltage stability of the system. This study highlights voltage stability issues of different generation technologies.

Considering a large power system, optimal power flow (OPF) optimally schedules all generators including wind generators. Uncertainty of wind power output can create significant active power generation mismatches of this OPF generation schedule. Incorporating uncertainty of generation, stochastic unit commitment method is described in Zhang et al. (2014). This method allows dynamic reserve scheduling for the uncertain generation technologies. However, to compute effect of forecast uncertainty on system voltage stability by solving OPF for several forecast error scenarios is very cumbersome.

As many units of wind farms are online, increased levels of wind penetration have generated a widespread concern over the impact on power system performance (SMITH et al., 2007). There are primarily two reasons for such a concern: 1) the variability of wind and, 2) the

nature of wind generators that is different from conventional generators (SHORTT et al., 2013). The effect of high wind penetration levels on the system performance becomes critical in the planning of future units and to accomplish the required level of renewable portfolio. Because of the variable nature of outputs of wind farms, many challenges are being faced by grid operators.

Traditionally, wind power is an energy source but not a capacity source (SMITH et al., 2007). This variability and uncertainty in the output of a large wind plant can be covered by reserve power of fast-acting dispatchable sources, such as natural gas turbines or hydro generators.

The impact of variability, particularly with reference to wind power, has been studied and documented extensively in recent years (RESTREPO; GALIANA, 2011; ORTEGA-VAZQUEZ; KIRSCHEN, 2010; UMMELS et al., 2007) by considering systems with and without variable generation. Nevertheless, over the time, wind generation penetration will alter the generation mix in the power systems. In order to maintain the system stability in such situations, an efficient method of stability analysis is needed.

Probabilistic analysis of power system small-signal stability was firstly proposed in (BURCHETT; HEYDT, 1978) to consider the influence of uncertainty in system parameters, which is approximately introduced from several sources subject to the multivariate normal distribution. The studies (BU et al., 2012) of probabilistic analysis to investigate the impact of stochastic uncertainty of grid-connected wind generation on power system small-signal stability.

1.3 MOTIVATION OF THIS THESIS

As explained above, wind integration into the power system has many challenges. In this thesis, the main challenge is the need for mathematical models for voltage stability analysis of wind energy into power systems. Thus, a relationship between voltage stability and uncertainty of wind generation is sought. Therefore, the objectives of this PhD research focus on addressing this challenge.

1.4 OBJECTIVES

In this thesis, a new and efficient method for determining the effect of wind power forecast errors on Minimum Singular Values (MSV) is developed and presented.

Regarding the proposed method, the wind generation forecast errors are included into the formulation and hence for estimating singular values.

Accordingly, assessing voltage stability of the system becomes a much efficient and simpler process. In order to verify the formulation, test studies were conducted considering the proposed method and comparable results also were obtained by solving OPF several times considering various forecast error scenarios. A comparison of results of these two methods is also given in this work.

1.5 ORGANIZATION OF THIS THESIS

This Chapter presents an introduction to the thesis and reviews literature related to wind power integration into the power system. It also gives introductions to different theoretical and mathematical concepts used in the study.

In Chapter 2 presents an overview of wind energy in the world and in Brazil. The wind potential in Brazil is presented. In parallel, the evolution of the Brazilian energy matrix and power generation is presented, as well as the current situation of the country in relation to wind power. In this chapter, an analysis of wind development around the world is also conducted.

In Chapter 3, a detailed explanation of the relationship between voltage stability and the singular values is presented. Likewise, the analytic methods and modeling techniques used to characterize the wind power output uncertainty on voltage stability using singular value analysis are described.

In chapter 4, after building mathematical models in Chapter 3, the wind uncertainty models are implemented in system power flow algorithms in Matlab environment. The IEEE 6-bus, IEEE 57-bus, IEEE 118-bus, The Southern Brazilian Reduced and an actual 581-bus systems are used for this analysis. Several studies at different operating points were completed for this purpose. Comparison of MSV and $\Delta\Sigma$ is also given in this chapter.

In Chapter 5 presents the conclusion of the thesis. Besides the summary of the complete study, contributions made by the work are also underlined.

1.6 CHAPTER SUMMARY

This chapter provided an introduction to the challenges faced in the integration of wind generators with power systems, in particular, the voltage instability problem. A survey for those challenges was presented. Research aims in this thesis were also identified and presented.

2 PANORAMA OF WIND POWER IN BRAZIL AND THE WORLD

After presenting the concepts that explain the inherent principles of stability of the power system, and the major challenges for the integration of wind generators, it is important now to contextualize the panorama of wind energy in Brazil and worldwide. Therefore, this chapter presents the global installed capacity, the capacity factors of wind farms installed in major countries. In parallel, it analyzes the projections of the future market for wind energy.

Subsequently, the focus of the chapter turns to the panorama of wind power in Brazil. So, initially the wind power potential of the country is shown, as well as its characteristic complementation with the hydroelectric sources. Thereafter, the growth of wind power is demonstrated. In addition, the evolution of the Brazilian energy matrix and the current situation is presented according to data released by the National Agency of Electrical Energy - ANEEL.

2.1 WORLD

Like hydropower, wind power has been used for thousands of years with the same objectives, namely: pumping water, grinding grains and other applications involving mechanical energy. The first wind powered electricity was produced by a machine built by Charles F. Brush in Cleveland, Ohio in 1888. It had a rated power of 12 kW (direct current - dc). Direct current electricity production continued in the form of small-scale, stand-alone (not connected to a grid) systems until the 1930's when the first large scale AC turbine was constructed in the USA. There was then a general lull in interest until the 1970's when the fuel crises sparked a revival in research and development work in North America (USA and Canada) and Europe (Denmark, Germany, The Netherlands, Spain, Sweden and the UK). The first commercial wind turbine connected to the public power grid was installed in 1976 in Denmark.

Modern wind turbine generators are highly sophisticated machines, taking full advantage of state-of-the-art technology, led by improvements in aerodynamic and structural design, materials technology and mechanical, electrical and control engineering and capable of producing several megawatts of electricity.

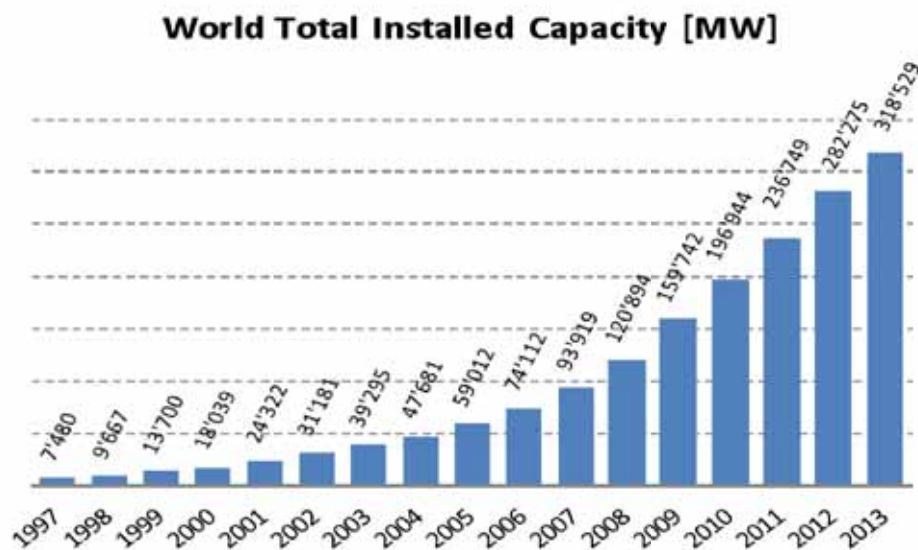
During the 1980's installed capacity costs dropped considerably and wind power has become an economically attractive option for commercial electricity generation. Large wind farms or wind power stations have become a common sight in many western countries. In this regard, the evolution of the global installed capacity of wind power, the evolution of wind

turbines and the capacity factors, as well as the projected growth of wind energy for the future are presented.

2.1.1 Current Capacity

At the end of the year 2013, the global installed capacity stemmed from the wind-source reached the milestone of 318,000 MW, which currently serves about 4% of global power demand. This strong representation of wind power was achieved through a decade of exponential growth in the industry. Figure 1 shows the installed capacity in the world between the years 1997 and 2013.

Figure 1 – World Total Installed Capacity



Source: World Wind Energy Association- WWEA (2014).

The global wind energy market installed only in 2011, 2012, and 2013 are about 39, 44, and 35 GW, respectively, which is a milestone in terms of annual capacity added, as can be seen in Figure 2.

Figure 2 – World Total Installed Capacity

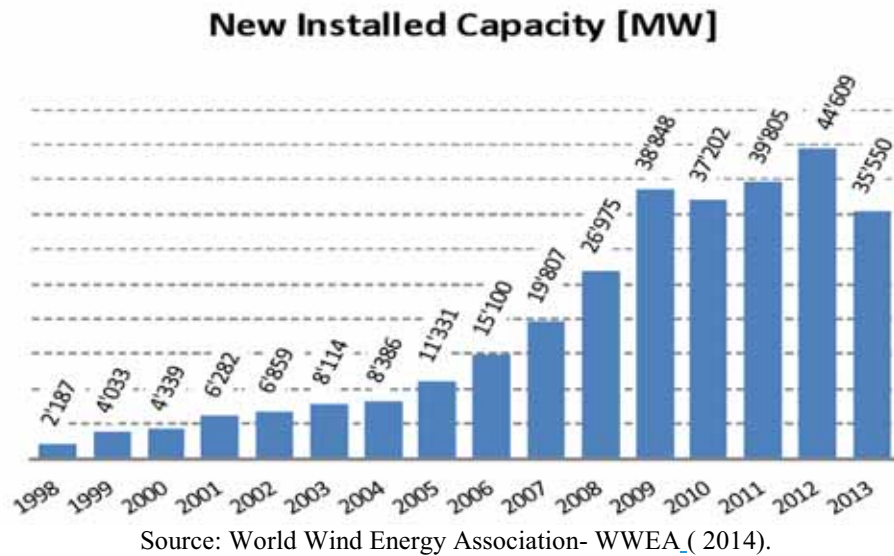


Figure 3 shows the high annual growth rates of source wind. The sector suffered in recent years, the effects of the global economic crisis started in late 2008, especially large wind markets as the case of the USA and Europe. However, though with a decline in the growth rate compared to the strong rate seen in previous years (in 2009, for example, 31.7%), the industry still maintained a considerable dynamism and growing.

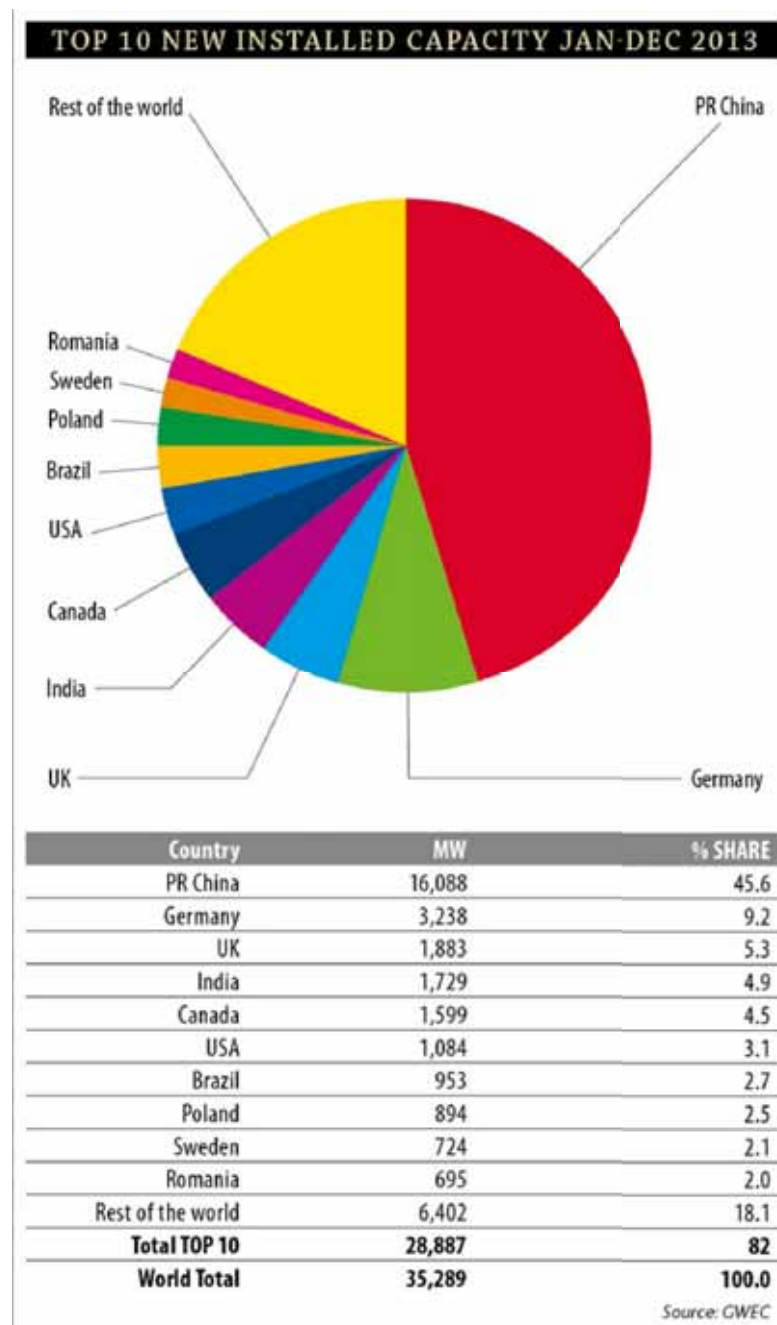
Figure 3 – World Market Growth Rates



Among the countries that have contributed towards increasing the capacity of global installed wind power in recent years, stands out China, was mainly responsible in terms of increase in installed capacity. Preliminary data indicate that China installed during the year

2013 approximately 16 GW of new wind turbines, i.e., more than 45% of the total new installed capacity worldwide (35.3 GW in 2013). The second major market for wind power was Germany, with an added capacity of 6.2 GW, followed by UK (1.8 GW), India (1.7 GW) and, surprisingly Canada (1.6 GW) that gained greater representation in the global market in this sector, and overtook the mighty USA market (1 GW). Brazil, Poland, Sweden and Romania added less than 1 GW each. Figure 4 shows the new installed capacity reached in late 2013 by country.

Figure 4 – New Installed Capacity 2013

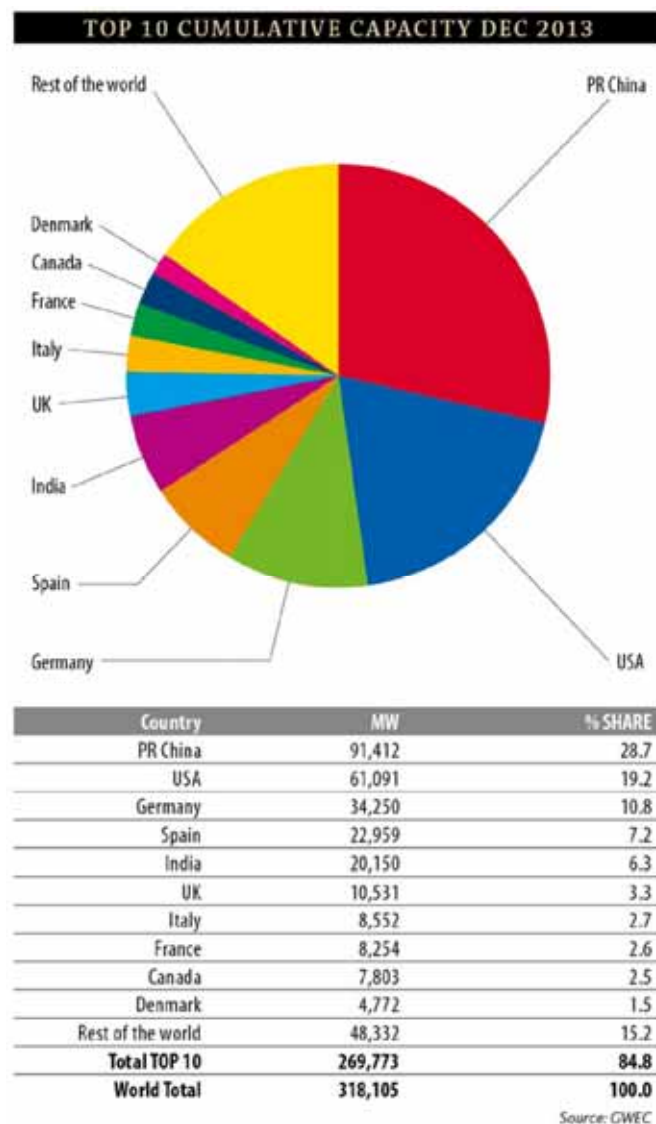


Source: Global Wind Energy Council- GWEC (2014).

Figure 5 shows, in percentage terms, and by country, the installed capacity at the end of year 2013. Thus, it is possible to observe that China has today more than a quarter of the world's installed capacity and was responsible for nearly half of the incremental installed capacity in 2013 (according to Figure 3), thus reaching the mark of 91GW of installed capacity, i.e., more than one quarter of the total global installed capacity (318 GW in 2013).

The second major market for wind power is still the USA, where almost a fifth of the total installed capacity to 61 GW is found; Germany, with 34 GW, occupies the third position. Other European countries also stand out with Spain, UK, Italy, France, and Denmark. India reached the fifth position (20 GW), and stands out as an emerging country, and Canada appears to highlight current 7.8 GW of installed capacity.

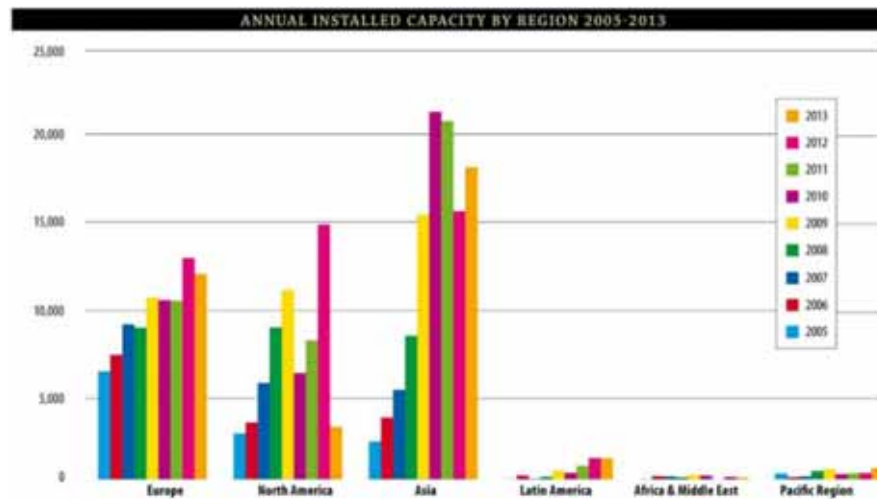
Figure 5 – Total Installed Capacity 2013



Source: Global Wind Energy Council- GWEC (2014).

Figure 6 shows the dominance of wind for different regions of the world markets, and that the supremacy of markets from China, USA, and Germany, is reflected in the sampling regions.

Figure 6 – Annual Installed Capacity for Region 2005-2013



Source: Global Wind Energy Council- (GWEC (2014).

2.1.2 Capacity factor

Capacity factor is an indicator of how much energy a particular wind turbine makes in a particular place, in technical terms, the ratio of the actual energy produced in a given period, to the hypothetical maximum possible, i.e. running full time at rated power.

All power plants have capacity factors, which vary depending on resource, technology, and purpose. Typical wind power capacity factors are 20-40%. Hydro capacity factors may be in the range of 30-80%, with the USA average toward the low end of that range. Photovoltaic capacity factors in Massachusetts are 12-15%. Nuclear capacity factors are usually in the range of 60% to over 100%, and the national average in 2002 was 92%. The capacity factors of thermal plants cover a wide range; base-loaded thermal power plants (e.g. large coal) may often be in the range of 70-90%, and a combined cycle gas plant might be 60% depending on gas prices, whereas power plants in the role of serving peak power loads will be much lower. One might expect a new biomass thermal plant to have an 80% capacity factor. (COMMUNITY WIND FACT SHEET SERIES, 2003).

Wind power plants have a much lower capacity factor but a much higher efficiency than typical fossil fuel plants. A higher capacity factor is not an indicator of higher efficiency, or vice versa.

The wind does not always blow; sometimes a wind power plant stands idle. Furthermore, wind power is not “dispatchable” – you cannot necessarily start it up when you most need it. As wind power is first added to a region’s grid, it does not replace an equivalent amount of existing generating capacity – i.e., the thermal generators that already existed will not immediately be dismantled.

Wind turbine technology has changed a lot in the past twenty years. Where a 600 kW faceplate capacity wind turbine of twenty years ago might have a 20-25% capacity factor, a modern 3 MW faceplate capacity wind turbine might have a 40% capacity factor in reasonably good wind resource locations and 47%+ in the best wind resource locations. In a 2008 study released by the U.S. Department of Energy's Office of Energy Efficiency and Renewable Energy, the capacity factor achieved by the U.S. wind turbine fleet is shown to be increasing as the technology improves. The capacity factor achieved by new wind turbines in 2010 reached almost 40%.

2.1.3 Projections of the future market for wind energy

This section aims at presenting and analyzing the results of the projection growth of wind energy. In this sense, the approach is the projected short- and long-term elaborated main institutions involved in this event.

2.1.3.1 Market Forecast for 2014-2018

The GWEC believes the market diversification trend that has emerged over the past several years and strengthened during 2013 to continue to do so over the next several years. New markets outside the OECD (Convention on the Organisation for Economic Co-operation and Development) continue to appear, and some of them will begin to make a significant difference to general market figures. Inside the OECD, as wind power approaches double digit penetration levels in an increasing number of markets, and as demand growth either stalls or goes backwards, incumbents feel increasingly threatened. The fight for market share and policy support in these markets is becoming more and more intense. As a result, most of the growth in the coming years will be in markets outside the OECD.

Today, in the absence of a concerted effort to combat climate change, it is wind has cost competitiveness that is its greatest advantage in the market place. In Brazil, South Africa, Turkey, Mexico and elsewhere, wind is competing directly and successfully with heavily

subsidized incumbents – so successfully in fact that in an auction last year in Brazil, wind power was excluded to ‘give the other energy sources a chance’.

Wind is coming in about 30% cheaper than the notorious giant World Bank financed coal-fired power plants in South Africa, while tell of PPAs (power purchase agreement) are signed for wind power in the US as low as US\$ 20/MWh; which of course translates into about US\$ 42 with the PTC (Production Tax Credit), but still extremely competitive (GLOBAL WIND ENERGY COUNCIL- GWEC, 2014).

The 2013 market saw China back on top, installing about five times as much wind power as Germany in the number two spot. The 2012 market leader, the US, dropped back to sixth place, behind Canada (which had a record year), and just ahead of Brazil. Despite a lackluster year, India moved into fourth place, right behind the UK, which had a good year both on and offshore. (Information that were shown in item 2.1.1).

When the projections were done for the 2013-2018 market two years ago, there were underestimates, as the drop in the US market by about 3 GW; but because of the nature of the PTC re-authorisation and the strong pipeline of new projects, the projection now looks to make up that 3 GW in 2014. Overall, 2014 looks to be a record year, with annual market growth of about 34%, to bring the annual market to about 47 GW, with strong installations in North America and Asia, and the Brazilian market really beginning to come into its own. South Africa, Brazil and Mexico will figure increasingly strongly in the annual market figures in the years to come. After 2014, the market prospect to return to a more ‘normal’ annual growth of 6-10% out to 2018. Cumulative growth will rise to nearly 15% in 2014, but average 12-14% from 2015 to 2018. Total installations should nearly double from today’s numbers by the end of the period, going from just over 300 GW today to just about 600 GW by the end of 2018. (GWEC, 2014)

Figure 7 – Market Forecast for 2014-2018



Source: Global Wind Energy Council- GWEC (2014).

Although there is a great interest in markets with large projections growth rates over the next five years, such that Latin America and Africa, most of the global market will continue in Asia, Europe and the United States.

Despite the low expected growth rate for Asia, compared with its growth in recent years, this will remain the largest market worldwide, as can be seen in Figure 8. The Chinese market reached a degree of stabilization and thus much of the growth of the Asian continent should come from India, with projections to reach the milestone of 5 GW per year by 2015. In parallel, there is an expectation about considerable growth of wind energy in Japan as there is a great effort in the country to replace its strongly focused nuclear plants after the accident in Fukushima with renewable energy sources. In this sense, the Japanese government has inducing offshore wind energy in the country.

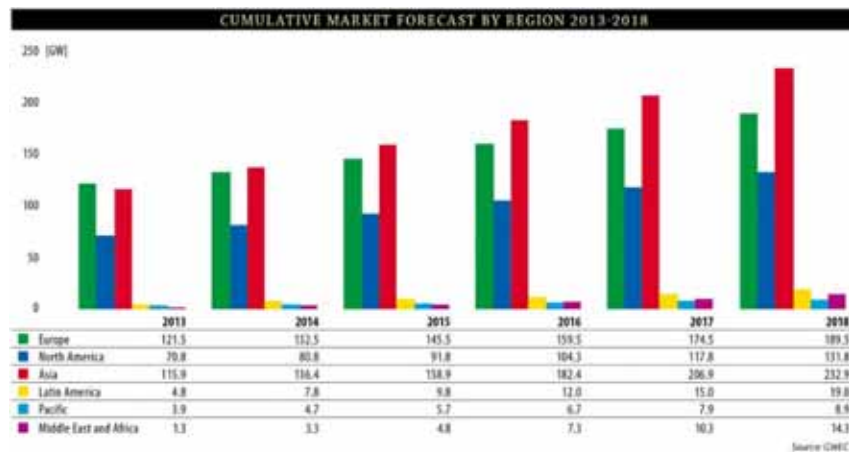
Figure 8 – Annual Market Forecast by Region for 2013-2018



Source: Global Wind Energy Council- GWEC (2014).

Meanwhile, Korea also tends to become an important player in the offshore market. Moreover, it should also be noted that Mongolia has built its first wind farm in 2012 and, despite a huge potential in the country, it does not expect a representative growth until the year 2018. Therefore, as can be seen in Figure 9, Asia should install 232 GW until 2018, an amount well above the capacity added in any other region, and thus it is expected to surpass Europe in terms of installed capacity by the year 2013 and reach a plateau 200 GW of installed capacity in 2017.

Figure 9 – Cumulative Market Forecast by Region for 2013-2018



Source: Global Wind Energy Council- GWEC (2014).

In the consolidated European market, Germany stood out in 2011 with strong growth. In parallel, the decision of the German government to replace all its nuclear plants by the year 2020 will cause the country to be a driver of wind power on the continent. It is projected to install 65 GW between the years 2014 and 2016 in Europe, which would reach the continent level of 160 GW in installed capacity in 2016; is noteworthy also regular growth of the offshore wind market in the region, a fact that will make the technology develop and earn a role increasingly prominent on the continent.

The North American market (including Mexico), is projected to increase installed capacity of around 50 GW in 2013-2016, which would make the region reach 100 GW of installed capacity at the end of 2016, approximately half of the installed capacity projected to Asia in 2016. For 2018, it expects 130 GW.

The Latin American market is led by Brazil, which has become an important global player to present a significant growth of building wind farms, as well as the main attraction of large manufacturers of wind turbines. The goal is to provide equipment for the robust Brazilian market as well as to supply the region of southern cone. In the South American continent, some

countries, such as Chile, Argentina and Uruguay, should contribute to the growth of wind in the region, although about three quarters of the projection of 8.6 GW to be installed in 2012-2016 period should be strong and detached from the Brazilian market. Thus, the region is expected to reach a level of 19 GW in 2018.

In Africa and the Middle East, the region observed a scene that is very little dynamic in 2011, with an increment of only 0.1 GW of installed capacity that year, as can be seen in Figure 7. However, it is projected to have an increment of 8 GW to be installed in 2012-2016, which will make the installed capacity in the region reach 14 GW in 2018. This highlights the growth expected in Egypt and Morocco, and especially in South Africa, which should have one increment of at least 400 MW per year in this decade.

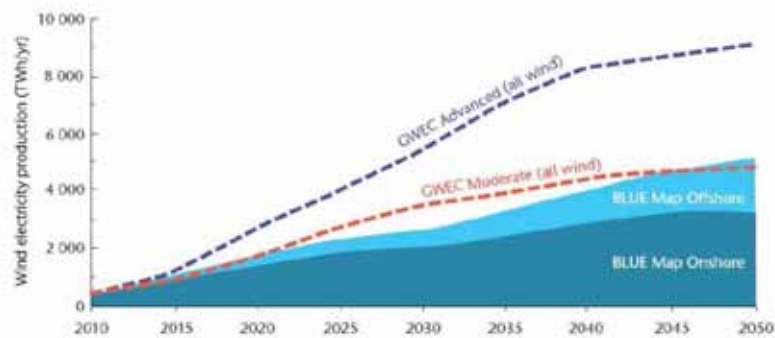
Finally, in the Pacific region, it is projected to have an increment in installed capacity more than 5 GW between 2012 and 2016, reaching approximately 9 GW in 2018, highlighting the growth of Australia and small but dynamic market in New Zealand.

2.1.3.2 Long-Term Market Forecast

The BLUE Map scenario also brings significant security of supply benefits to all four countries or regions, particularly through reduced oil use. In the United States and OECD Europe, oil demand in 2050 is between 62% and 51% lower than 2007 levels (gas demand shows similar declines). In China and India, oil demand still grows in the BLUE Map scenario, but is between 51% and 56% lower by 2050 than in the Baseline scenario. (INTERNATIONAL ENERGY AGENCY- IEA, 2010).

According to the IEA Roadmap suggested by the wind industry, wind energy will experience tremendous growth in the coming decades, reaching an annual production approximately 2,600 TWh in 2030 (stemmed from an installed capacity of 1,000 GW), representing about 9% of global electricity consumption, and 5,100 TWh in 2050 (stemmed from an installed capacity above 2,000 GW), which represent about 12% of global electricity consumption. Market projections indicate further growth if an optimistic scenario is considered (5,400 TWh in 2030 and 9100 TWh in 2050), indicated by the curve GWEC Advanced (All Wind) in Figure 10.

Figure 10 – Wind energy in Blue map of IEA/ GWEC



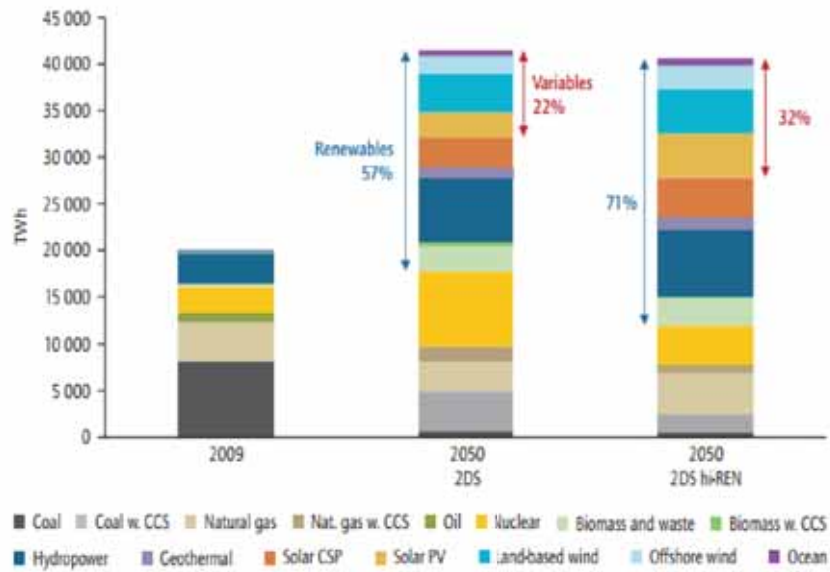
Source: Global Wind Energy Council- GWEC (2014).

Wind power could generate up to 18% of the world's electricity by 2050, compared with 2.6% today, according Technology Roadmap. The almost 300 gigawatts of current wind power worldwide must increase eight- to ten-fold to achieve the roadmap's vision, with more than \$ 78 billion in investment in 2012 progressively reaching \$ 150 billion per year.

This roadmap has as a starting point of the vision from the IEA ETP 2012 analysis, which describes diverse future scenarios for the global energy system in 2050.

A Base Case Scenario, which is largely an extension of current trends, projects that energy demand will almost double during the intervening years (compared to 2009) and associated CO₂ emissions will rise even more rapidly, pushing the global mean temperature up by 6°C (the 6°C Scenario [6DS]). An alternative scenario sees energy systems radically transformed to achieve the goal of limiting global mean temperature increase to 2°C (the 2°C Scenario [2DS]). A third option, the High Renewables Scenario (hiRen Scenario), achieves the target with a larger share of renewables, which requires faster and stronger deployment of wind power to compensate for the assumed slower progress in the development of CCS (carbon capture and storage) and deployment of nuclear than in 2DS. This hiRen Scenario is more challenging for renewables in the electricity sector. (IEA, 2013). Figure 11 shows the generation of electricity from renewable sources by 2050.

Figure 11 – Global electricity mix by 2050 in the 2DS and hiRen scenario

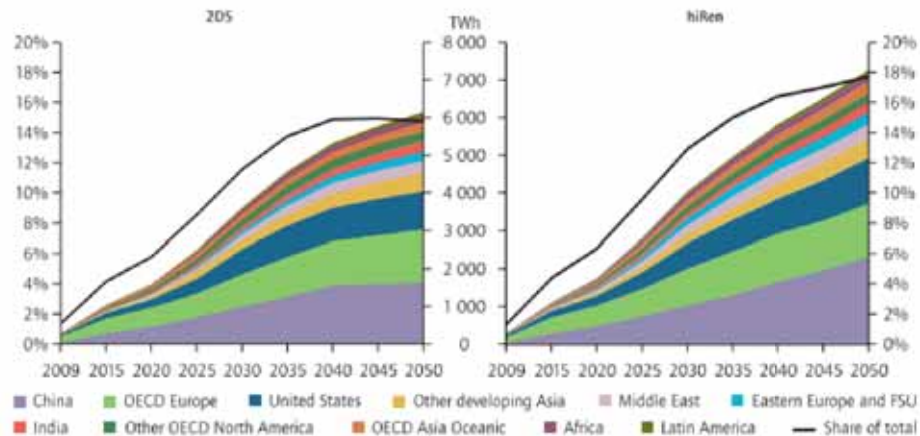


Source: International Energy Agency- IEA (2012a).

To accomplish the goals set out in the 2DS and hiRen Scenarios, it is necessary in this update to increase considerably the wind capacity deployment that was envisioned in 2009. Against the initial wind roadmap, the 2DS now sees a deployment of 1 400 GW in 2030 (compared to 1 000 GW) and 2 300 GW in 2050 (compared to 2 000 GW). In terms of electricity generation, the 2DS forecasts 6 150 TWh in 2050 (almost a 20% increase), so that wind achieves a 15% share in the global electricity mix (against 12%). Wind capacity in the hiRen Scenario reaches 1 600 GW in 2030 and 2 700 GW in 2050, and generates 7 250 TWh, almost a one-fifth increase compared to the 2DS. In this scenario, the share of wind power in electricity generation increases to 18% in 2050. The higher penetration of wind in the hiRen is driven by a lower deployment of both CCS and nuclear power.

Figure 12 shows the scenario where China will overtake OECD Europe as the leading producer of wind power, by 2020 in the 2DS and by 2025 in hiRen; in both cases, the United States will be the third-largest market. India and other developing countries in Asia emerge by 2020 as an important market. By 2050, China leads with 1 600 TWh to 2 300 TWh, followed by OECD Europe (1 300 TWh to 1 400 TWh) and the United States (1 000 TWh to 1 200 TWh), and then by other developing countries in Asia and the Middle East.

Figure 12 – Regional production of wind electricity in the 2DS and hiRen



Source: International Energy Agency—IEA (2012a).

However, it is important to note that there are many uncertainties in these studies that seek to make inferences about the future. In this sense, it is notable that a change of technology standard, such as, for example, a troublesome innovation of some technology, can generate a large rearrangement in the world's energy sources.

2.2 BRAZIL

The Brazilian wind potential for energy recovery has been the subject of studies since the 1970s and its history reveals a slow but progressive unveiling of a natural energy potential relevant magnitude existing in the country. Although Brazil experienced a great development in wind power, the last official document about the potential for exploitation energy through winds is the Atlas of Brazilian Wind Power Potential, published in 2001. This atlas estimated potential energy through wind power 143.5 GW (272.2 TWh / year), based on measurements at a height of 50 m, of which 75 GW (144.3 TWh / year) are located only in the Northeast. However, most current studies, but still unofficial, indicate a higher potential of 300 GW, since the current technology allows the installation of wind turbines on towers over 100 feet tall, which allows larger area sweep of blades, greater local speeds, and winds that are more constant.

Although Brazil has huge potential for the use of wind power, largely due to the good quality of its winds, the recent history of sector development in the country is incomparable to the growth of wind power in several European countries and the United States, for example.

It was in 1992 that Brazil had the installation of the first wind turbine through a project of CELPE (Electric Power Center from Pernambuco), in the archipelago of Fernando de Noronha

(Pernambuco) with a capacity of 75 kW, enough to supply 10% of the consumption of the island at that time.

During the next ten years, however, little progress has been made in the consolidation wind power as an alternative power generation in the country, partly due to lack of policies, but mainly because of the high cost of technology.

During the energy crisis of 2001 there was an attempt to encourage the hiring of generation of wind power in the country. Then, the Emergency Program for Wind Energy – PROEÓLICA was created. This program aimed to build 1,050 MW of wind energy projects until December 2003. It was then spoken of seasonal complementarity of wind regime with hydrological flows in hydroelectric reservoirs. This program, however, lead to no results, and was replaced by the PROINFA (Program of Incentives for Alternative Electricity Sources).

Besides encouraging the development of renewable sources in the energy mix, PROINFA paved the way toward the establishment of wind turbines and components industry in the country.

In late 2009, the Second Power Reserve Auction, which was the first auction sale of energy focused exclusively on wind power, started. The Reserve Auction Energy hires an amount of energy more/less than that estimated to meet the demand of the country as a store of Assured energy to the electrical system.

The Second Power Reserve Auction was a success with hiring 1.8 GW and opened doors to new auctions that occurred in the following years. In August 2010, the Third Power Reserve Auction and Alternative Sources Auction, which contracted 2GW of wind power, started. These auctions not only worked more with the wind model, but also contemplated various renewable sources competing to negotiate their energy in the auction. In 2011, there were already three more auctions, 4th READ, A-3 and A-5 where wind power has great prominence to negotiate the total of 2.9 GW. Finally, in December 2012, the A-5 auction contact energy to supply beginning in 2017. In this auction 281.9 MW were contacted.

Besides PROINFA and auctions, wind power also markets its energy on a smaller scale in the free market where contractual terms are freely negotiated between counterparties.

Because of PROINFA of auctions and the free market, by the end of 2012, Brazil has 108 wind farms totaling 2.5 GW of installed capacity.

The curve of the installed capacity of wind power demonstrates the virtuous supply growth over the years. The composition of the data is done by consolidating the contracted capacities in free and regulated employment environments, respectively. At the end of 2018,

there will be 14.4 GW installed in Brazil. Figure 13 shows the new and accumulated installed capacity in Brazil.

Figure 13 – Installed capacity in Brazil



Source: Associação Brasileira de Energia Eólica- ABEólica (2014).

The states of Ceará, Rio Grande do Sul, Rio Grande do Norte, Bahia and Santa Catarina have the most installed capacity in commercial operation. In addition, in January 2014, the Ceará, with its 20 plants, had the greatest generation, reaching the second highest factor average capacity for the month, 43%. The state with the largest capacity factor was Bahia, with 45% and 8 plants.

Despite having the largest installed capacity, the Rio Grande do Norte still has a capacity of 534 MW plants of the 2nd Auction of Alternative Sources (LFA) and 54 MW of plants in the 2nd and 3rd Auctions Reserve Power (LER). National Electric Energy Agency considers that the conditions for entering into operation trade, but due to restriction on distribution and / or transmission system for connection to SIN, systems were delayed. In December 2013, in Rio Grande do Norte, 324 MW of power plants in the auctions of Reserve cited that in January 2014 the operation of generating units under test began.

In Bahia, there are 252.2 MW capacity power plants for the 2nd LER and 60 MW of power plants considered for the 2nd LFA, ANEEL as suitable, but were the same situation restriction interconnection to SIN as noted earlier, these plants are not considered in the analyzes presented.

The outlook for the end of 2017 indicates 8.7 GW of wind power in operation in the Brazilian energy matrix.

2.3 CHAPTER SUMMARY

This chapter provided a panorama about the wind power around the world with special focus on Brazil. Various data and graphs were presented demonstrating the strong growth of wind power in recent years.

3 PROPOSED METHOD OF ANALYSES OF VOLTAGE STABILITY

This chapter presents a schematic illustration of the proposed system for analysis of the voltage stability of power systems, which will be addressed in this research.

The Working Group of the Institute of Electrical and Electronics Engineers (IEEE WORKING GROUP, 1990) has developed a set of definitions and solving techniques associated with the problem of voltage stability of power systems, such as, the voltage instability occurs due to an attempt of the power system to answer the load beyond the combined capacity of transmission and generation.

The operation of the system does not have control over the evolution of the load because it is associated only with intention of the consumer. The system has obligation to answer this demand. Moreover, when this situation is compromising the integrity (security) of the system, preventive and emergency measures should be taken, e.g., load shedding, when there is no other plausible alternative.

To avoid these disorders, it is necessary to carry out some security estimates and develop preventive strategies. In fact, this research aims at the development of a methodology for the analysis of voltage stability.

3.1 VOLTAGE STABILITY AND MINIMUM SINGULAR VALUE OF SYSTEM JACOBIAN

This section presents the technique for calculating the minimum singular value (MSV) of the load flow Jacobian. The Singular Value Decomposition is a method of orthogonal decomposition used in algebra, which has the enormous advantage that singular values are calculated; therefore, the method is well-conditioned.

The singular values and their corresponding vectors provide information about system condition at the critical operating point. Such information includes the point of collapse and the singularity of Jacobian matrix. More importantly, since voltage stability is correlated with the singularity of Jacobian matrix [LÖF et al., 1992], application of such analysis can provide indicators of voltage stability.

3.1.1 Minimum Singular Value Methods

The problem of OPF, which aims at minimizing the total operation cost, is formulated as:

Minimize Generation Cost:

$$f(\text{PG}) \quad (1)$$

Subject to:

Bus power balance equations as below for all buses:

$$\text{PG}_i - \text{PD}_i - P_i(\mathbf{V}, \delta) = 0 \quad i \in 1 \text{ to NB} \quad (2.1)$$

$$\text{QG}_i - \text{QD}_i - Q_i(\mathbf{V}, \delta) = 0 \quad i \in 1 \text{ to NB} \quad (2.2)$$

The problem in (1) and (2) is constrained by limits on the generator power (PG) and bus voltage (V). Linearizing the above equations around an operating point (V, δ), one may write:

$$\begin{bmatrix} \Delta \mathbf{P} \\ \Delta \mathbf{Q} \end{bmatrix} = \begin{bmatrix} \mathbf{J}_1 & \mathbf{J}_2 \\ \mathbf{J}_3 & \mathbf{J}_4 \end{bmatrix} \begin{bmatrix} \Delta \delta \\ \Delta \mathbf{V} \end{bmatrix} \quad (3)$$

By optimizing real power generation to minimize total costs for the current load on the system (1) and (2) provide the optimal state, i.e., the optimal power generation schedule. In this optimal state as determined by OPF, system Jacobian matrix is evaluated. In case of wind generator forecast errors, it is assumed that reactive power outputs are not affected. Hence, setting $\Delta \mathbf{Q} = [0]$, (3) can be simplified as below:

$$\Delta \mathbf{P} = [\mathbf{J}_1 - \mathbf{J}_2 \cdot \mathbf{J}_4^{-1} \cdot \mathbf{J}_3] \Delta \delta = [\mathbf{J}_{\text{P}\delta}] \Delta \delta \quad (4)$$

Through the analysis of the decomposition of power flow, the Jacobian matrix shows direct relationship between $\Delta \mathbf{P}$ and $\Delta \delta$. However, in this study, the above reduced matrix of (4) will be used.

$$\Delta \mathbf{P} = [\mathbf{J}_{\text{P}\delta}] \Delta \delta \quad (5)$$

The Minimum Singular Value is obtained using dispersity techniques; so, it might find application in real time. One may factorize the system Jacobian to determine singular values [TIRANUCHIT; THOMAS, 1988]:

$$[J_{P\delta}] = [SU][\Sigma][SV]^T \quad (6)$$

Rearranging (6), considering a small perturbation around the previous state of $\Delta\delta$ and ΔV , the following can be written:

$$[J_{P+\Delta P, \delta+\Delta\delta}] = [SU + \Delta SU][\Sigma + \Delta\Sigma][SV + \Delta SV]^T \quad (7)$$

The LHS of (7) was expanded using Taylor's series and only the first order term of the series including the Hessian [H] is maintained, while overlooking the higher order terms, then:

$$[J_{P+\Delta P, \delta+\Delta\delta}] - [J_{P\delta}] = [H][\Delta\delta] \quad (8)$$

And, expanding RHS of (7) neglecting higher order terms, it can be re-written as:

$$\begin{aligned} [H][\Delta\delta] &= [\Delta SU][\Sigma][SV]^T + [SU][\Delta\Sigma][SV]^T \\ &+ [SU][\Sigma][\Delta SV]^T \end{aligned} \quad (9)$$

Imposing orthogonality constraints on the updated left and right singular matrices, one gets:

$$[SU + \Delta SU][SU + \Delta SU]^T = I \quad (10.1)$$

$$[SV + \Delta SV][SV + \Delta SV]^T = I \quad (10.2)$$

Expanding (10), disregarding the second order terms, and using the orthogonality property of [SU] and [SV], the matrices [SR] and [SL] were written as:

$$[SR] = [SU]^T [\Delta SU] = -[\Delta SU]^T [SU] \quad (11.1)$$

$$[SL] = [SV]^T [\Delta SV] = -[\Delta SV]^T [SV] \quad (11.2)$$

From (11), it can be seen that diagonal elements of $[SR]$ and $[SL]$ are zeros. Pre-multiplying and post-multiplying (9) with $[SU]^T$ and $[SV]$ respectively results in:

$$[SU]^T [H][\Delta\delta][SV] = [SR][\Sigma] + [\Delta\Sigma] + [\Sigma][SL] \quad (12)$$

Since $[SR][\Sigma]$ and $[\Sigma][SL]$ have zeros as their diagonal elements, Equation (12) is reduced to :

$$[\Delta\Sigma] = [SU]^T [H][\Delta\delta][SV] \quad (13)$$

According to Equation (13), estimating the changes in bus phase angles with respect to the minimum singular value of the power flow system Jacobian is allowed.

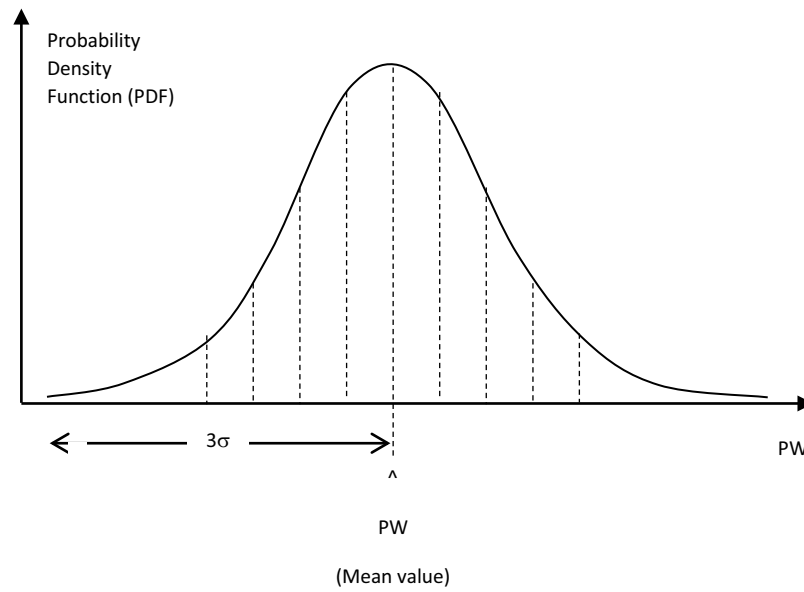
Uncertainties in wind forecast are used to estimate possible changes in real power output of wind generators. These real power output changes can be correlated to bus voltage angles using (4) and later changes in singular values using (13). Therefore, uncertainty of wind power forecasts can be used to determine changes in minimum singular value of the system Jacobian. The next section shows this proposed method.

3.2 EFFECT OF WIND POWER UNCERTAINTY ON VOLTAGE STABILITY

In this section, uncertainty in the power system voltage is considered as dependent upon the uncertainty of wind generation. Thus probabilistic distribution functions of wind generation are used to generate a probable event space. With this approach, the complete event space is considered for estimating the probability distribution of voltage solutions of all buses.

For this reason, wind power is forecasted for short term and used in 24-hour unit commitment, whereas optimal power flow algorithms are employed to determine the optimal generation schedule. In this process, the best forecast is used with a reasonable degree of risk. Typical forecasts of wind power assume that the forecast error is distributed as normal distribution in the short term horizon as shown in Figure 14 (HODGE; MILLIGAN, 2011).

Figure 14 – Normal distribution of wind power output forecast



Source: Hodg and Milligan (2011).

In each forecast, the mean value \hat{PW}_i provides the best estimate of wind power, while the uncertainty denotes confidence in wind power forecast. The wind power may be within $\pm 3\sigma_i$ of the forecast value, where σ_i is the standard deviation of the normal forecast.

Step 1: Optimal Power Flow

Optimal power flow formulation in (1) and (2) is solved using the mean value of wind power forecast, \hat{PW}_i .

Step 2: Determination of effect on MSV

Variations of wind power generation at bus i (PW_i) is modeled as a normal probability density function (Fig. 1) with respective mean values and variance values. The Probability Density Function (PDF) of PW_i at bus i is defined below:

$$\rho_i(PW_i) = \frac{1}{\sqrt{2\pi\sigma_i^2}} \exp\left(-\frac{\left(PW_i - \hat{PW}_i\right)^2}{2\sigma_i^2}\right) \quad (14)$$

Where ρ_i (PW_i) is the value of probability density for a real power output of PW_i . The PDF of PW_i within the interval of $\hat{P}W_i \pm 3\sigma_i$ has a probability of 0.997.

Using (5), change in bus voltage angles is evaluated as a function of forecast variance as below:

$$[\Delta\delta] = [J_{P\delta}]^{-1}[\Delta P] = [J_{P\delta}]^{-1}[3\sigma] \quad (15)$$

Using (13), the variance is related to change in minimum singular value as below:

$$[\Delta\Sigma] = [SU]^T [[H][J_{P\delta}]^{-1}[3\sigma]][SV] \quad (16)$$

This relation allows a system operator to estimate the effect of uncertainty of the wind power forecast on minimum singular values that gives an indication of the effect on voltage stability. In case where the system is operating in a stressed state, this tool can be used as an alarm.

The relationship derived above uses only a part of the Jacobian matrix. Therefore, it reduces the computational burden. Furthermore, it establishes a direct link between the uncertainty and the minimum singular values. This method was tested comparing singular values of full Jacobian matrix. Three different system studies are reported in the next section for this comparison.

3.3 CHAPTER SUMMARY

This chapter presented the mathematical model for the study effect of uncertainty of the wind power forecast on minimum singular values. These equations will be used for the simulations in the next chapter.

4 TEST AND RESULTS

In this chapter, the proposed method is demonstrated through numerical tests on the Ward and Hale 6-bus, IEEE 57-bus, IEEE 118-bus systems, the Southern Brazilian System, and an actual large system of 581 buses. In these test systems, demand and generation values were altered to stress respective transmission systems reducing their voltage stability margins to collapse and representing a possible situation with large scale renewable generation integration. The purpose of studying the variation of Minimum Singular Value model is only to show the efficiency of such tool for stability analysis in power systems.

4.1 DESCRIPTION OF TEST SYSTEMS

In the test systems, demand and generation values were altered to stress respective transmission systems in order to reduce their voltage stability margins.

As a result, the systems is forced to the collapse point of voltage stability by representing a possible situation with large-scale renewable generation integration.

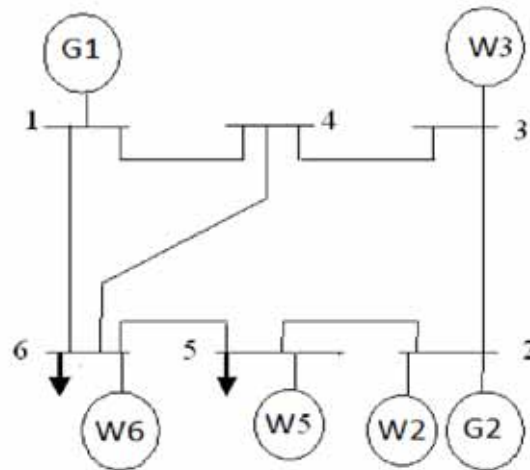
The criterion for wind generator allocation was to connect them at generator buses of the system in order to preserve the characteristics of the buses of the test system, i.e., no inclusion of new generation bus. For simulation purposes, five cases were considered. In the first case (base case), mean value of the wind power forecast ($\hat{P}W_i$) was used. In order to compute the effect of uncertainty of wind power output on MSV, four test cases with uncertainty of wind power defined by two ranges of standard deviations were considered ($3\sigma = 0.1 \times \hat{P}W_i$ and $3\sigma = 0.2 \times \hat{P}W_i$). In other words, four cases of $\pm 10\%$ and $\pm 20\%$ variations from the mean value or base case ($\hat{P}W_i$) were considered. Furthermore, it is assumed that wind power variations occurred simultaneously in all the wind generators installed in the test system. Individual variation of the wind generators will not be addressed in this work. The system was studied considering five wind generation cases equaling base case ($\hat{P}W_i$) and four cases ($0.8 \times \hat{P}W_i$, $0.9 \times \hat{P}W_i$, $1.1 \times \hat{P}W_i$, $1.2 \times \hat{P}W_i$). Using (16), variations in MSV were determined considering these change values of PW (ΔP).

However, for the simulations of the actual system, such deviation values were lowered due to the intrinsic characteristics of this system.

4.1.1 Ward and Hale 6-Bus System

Figure 15 shows the 6-bus System. The 6-bus System has 4 wind generators at buses 2, 3, 5 and 6. Both the number of wind generators, such as their locations, were taken randomly.

Figure 15 – The 6-Bus System



Source: The author

Table 1- Variation of $\Delta\Sigma$ of the 6-Bus Test System

$\Delta\Sigma$	Case PW- 20%	Case PW-10%	Case PW+10%	Case PW+20%
$\Delta\Sigma 1$	0.4844	0.2422	-0.2422	-0.4844
$\Delta\Sigma 2$	0.4357	0.2179	-0.2179	-0.4357
$\Delta\Sigma 3$	0.0886	0.0443	-0.0443	-0.0886
$\Delta\Sigma 4$	-0.0364	-0.0182	0.0364	0.0182
$\Delta\Sigma 5$	-0.0244	-0.0122	0.0244	0.0122

Source: The author

In order to verify these results, the OPF problem was solved five times. System Jacobian matrix was estimated for each case at the optimal state. MSV of the optimized system Jacobian are reported in Table 2.

Table 1 - Minimum Singular Values of the 6-Bus Test System

MSV	20% Reduced	10% Reduced	Base Case	10% Increased	20% Increased
SV1	6.554	6.3942	6.2345	6.0752	5.9167
SV2	4.2758	4.1533	4.0261	3.895	3.7688
SV3	4.0955	4.01	3.925	3.8401	3.7469
SV4	2.6232	2.6243	2.6243	2.6226	2.6189
SV5	1.0357	0.9576	0.8802	0.8038	0.7287

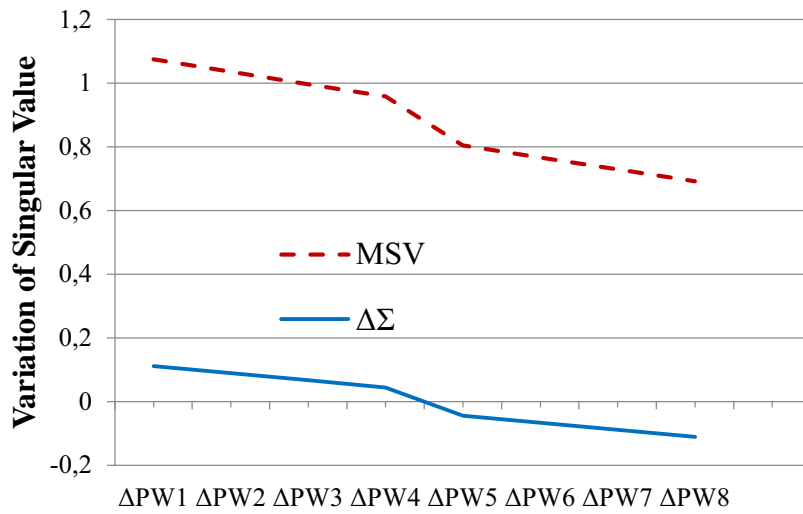
Source: The author

Even though the values are not equal due to errors caused by second order linearization, comparing Table 1 and Table 2, it can be clearly seen that the variation has the same trend. In other words, the behavior of the minimum singular value as it approaches the point of collapse (zero) is the same. The trend can be verified by analyzing the plots in Figure 16. The SV5, from Table 2, is the smallest MSV, whereas $\Delta\Sigma 5$, from Table I, is the smallest value of $\Delta\Sigma$, and their trend computed by using the proposed method is nearly identical to that estimated by solving OPF repeatedly. It should be noted that the change in the MSV ($\Delta\Sigma$) transitions through zero as the proposed method finds MSV at mean forecast value and computes changes in MSV with reference to the mean forecast value.

Clearly, it can be seen from Figure 16 that the minimum singular value SV5 (as seen from MSV) reduces with positive flow error indicating a reducing voltage stability margin. This is found by repeated OPF solutions. The corresponding analysis by the proposed method yields the change graph (additional operating points were simulated) via a single OPF solution and Hessian based sensitivity matrix, showing that the MSV reduces for an increase in PW (as seen from $\Delta\Sigma$). Hence, using the proposed method, with ease of computation and a linear relation, effect of uncertainty in wind generation is translated into effect on system voltage stability.

From Figure 16, the same trend was observed when analyzing the change in the MSV from both methods; however, it is evident that the proposed method shows more sensitive variations, In other words, the tendency to approach the collapse point sharply occurs. The proposed method is, therefore, suitable to analyze the effect of wind uncertainty on voltage stability of a power system.

Figure 16 - Minimum singular value versus $\Delta\Sigma$ for 6-bus system



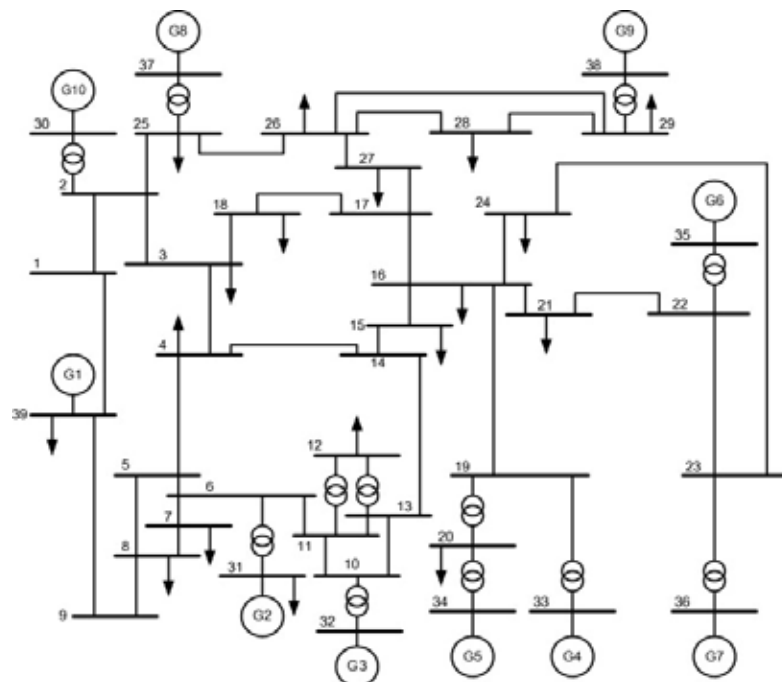
Variation of PW

Source: The author

4.1.2 IEEE 57-Bus System

Figure 17 shows the IEEE 57-bus system. In the 57-bus test system, 41 wind generators are assumed to be operating with existing generators in the system. Both the numbers of generators, and their locations, were randomly assigned.

Figure 17 - The 57-Bus System



Source: The author

Similar to the previous system, the 57-bus system was optimized considering base case and four other cases. In order to see the effect of variation of wind power on voltage stability, standard deviation of wind power outputs were assumed as: $3\sigma = \pm 0.1 \times \hat{PWi}$ and $3\sigma = \pm 0.2 \times \hat{PWi}$. With these uncertainty values, MSV and $\Delta\Sigma$ were determined using (16). Table 3 gives these variations of $\Delta\Sigma$.

Table 2 - Variation of Smallest $\Delta\Sigma$ of the 57-Bus Test System

$\Delta\Sigma$	Case PW- 20%	Case PW-10%	Case PW+10%	Case PW+20%
$\Delta\Sigma$ 52	-0.0467	-0.0234	0.0234	0.0467
$\Delta\Sigma$ 53	-0.045	-0.0225	0.0225	0.045
$\Delta\Sigma$ 54	-0.0378	-0.0189	0.0189	0.0378
$\Delta\Sigma$ 55	-0.0254	-0.0127	0.0127	0.0254
$\Delta\Sigma$ 56	0.0253	0.0126	-0.0126	-0.0253

Source: The author

The same five cases were used to analyze the MSV of the system Jacobian matrix (4). Table 4 shows the five smallest MSV obtained when above variations of power are assumed in the IEEE 57-bus test system.

Table 3 - Smallest MSV of 57-Bus Test System

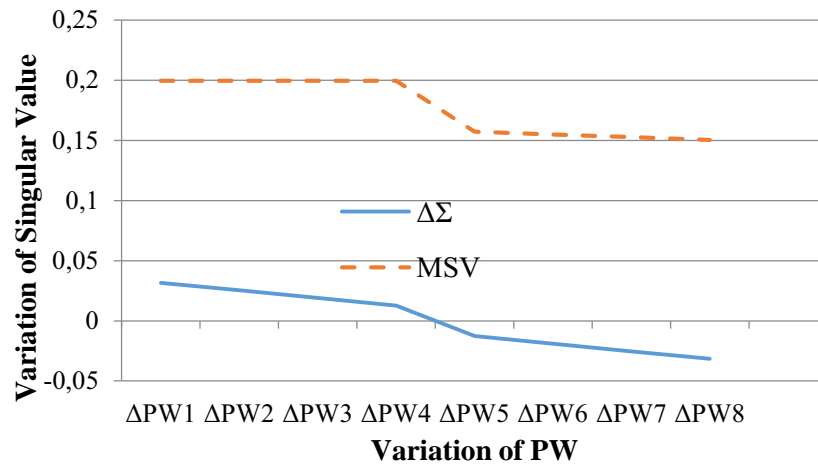
MSV	20% Reduced	10% Reduced	Best Forecast	10% Increased	20% Increased
SV52	0.7817	0.7817	0.6645	0.6599	0.6555
SV53	0.6528	0.6528	0.5615	0.5582	0.5547
SV54	0.4978	0.4978	0.4105	0.4046	0.3987
SV55	0.2749	0.2749	0.2271	0.2268	0.2265
SV56	0.1997	0.1997	0.1618	0.1573	0.1527

Source: The author

Comparing Tables 3 and 4, again it is clear that the trend of minimum singular values remains the same. This can be concluded by examining the behavior of the minimum singular and its trajectory to approach the point of collapse (zero). The trend can be verified by analyzing Figure 18. Apart from showing the same trend, the proposed method shows more sensitive variations. This proves the accuracy of proposed method. It is also evident that the trend shows

that a certain change in wind power output could cause voltage collapse when the transmission system is loaded more.

Figure 18 - MSV versus $\Delta\Sigma$ for 57- bus system

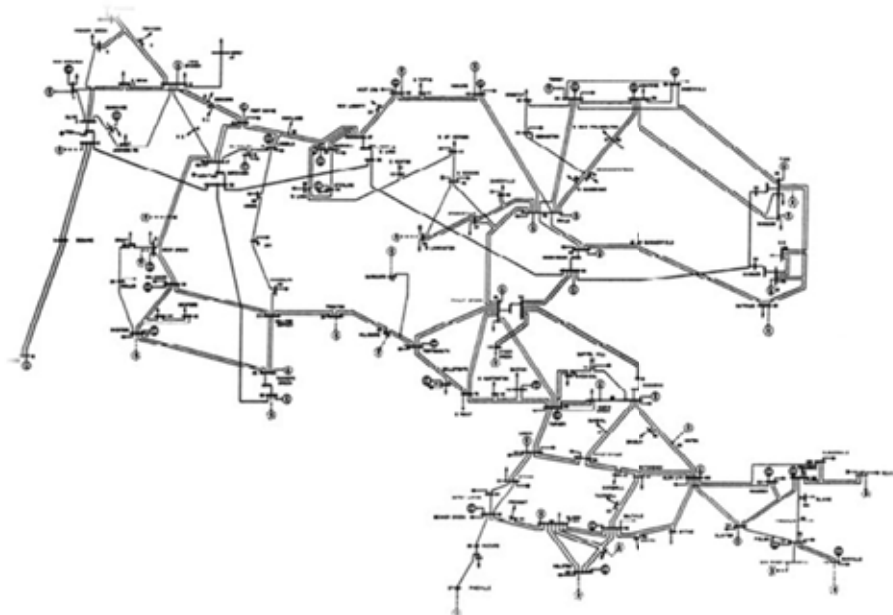


Source: The author

4.1.3 IEEE 118-Bus System

Figure 19 shows IEEE118-bus System. In this system, 91 wind generators were considered along with other 54 traditional generators. Both the bus number of wind generators and their locations were selected randomly.

Figure 19 - The IEEE 118-Bus System



Source: Power system test case archive (1996).

The same study was repeated for the IEEE 118-bus System. Similar to the previous systems, the 118-bus system was optimized considering a base case and four other test cases. Over again, to notice the effect of variation of wind power on voltage stability, standard deviation of wind power outputs were assumed as: $3\sigma = 0.1 \times \hat{PWi}$ and $3\sigma = 0.2 \times \hat{PWi}$. And again using (16), variations in minimum singular values were determined. These changes of $\Delta\Sigma$ are reported in Table 5.

Table 4 - Variation of Smallest $\Delta\Sigma$ of 118-Bus Test System

$\Delta\Sigma$	Case PW- 20%	Case PW-10%	Case PW+10%	Case PW+20%
$\Delta\Sigma$ 113	0.0069	0.0035	-0.0035	-0.0069
$\Delta\Sigma$ 114	0.0236	0.0118	-0.0118	-0.0236
$\Delta\Sigma$ 115	0.0388	0.0194	-0.0194	-0.0388
$\Delta\Sigma$ 116	0.0409	0.0205	-0.0205	-0.0409
$\Delta\Sigma$ 117	0.0552	0.0276	-0.0276	-0.0552

Source: The author

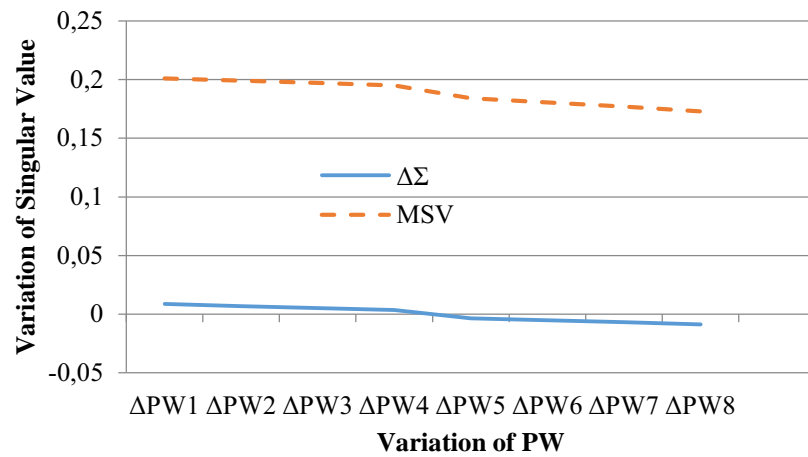
Similar analysis with the same wind generation cases and system Jacobian matrix was carried out. The results are given in Table 6.

Table 5 - Smallest MSV of 118 Bus Test System

MSV	20% Reduced	10% Reduced	Base Case	10% Increased	20% Increased
SV113	1.5132	1.5083	1.5024	1.4954	1.4872
SV114	1.1802	1.1798	1.1792	1.1784	1.1772
SV115	0.9305	0.9241	0.9148	0.9022	0.8862
SV116	0.3806	0.376	0.3709	0.3653	0.3591
SV117	0.1992	0.1951	0.1901	0.184	0.1769

Source: The author

Table 6 shows the five smallest singular values obtained when a variation of wind power is assumed in the 118-Bus System. Evidently, on reviewing Tables 5 and 6, it can be inferred that trend of singular values in the two tables are similar. The trend can be verified by inspection of Figure 20. This can be thus interpreted that on having an uncertainty in wind power forecast, the system voltage stability is affected considerably.

Figure 20 - MSV versus $\Delta\Sigma$ for 118 bus system

Source: The author

4.1.4 Southern Brazilian Reduced System

The Southern Brazilian Reduced System (MINUSSI, ~~and~~ ROMERO, 1990; MONTICELLI, 1994) has 10 generators, 45 buses and 73 transmission lines (the data of this system are in Appendix and its single-line diagram is shown in Figure 21).

Table 6 - Variation of Smallest $\Delta\Sigma$ of the Southern Brazilian Reduced System

$\Delta\Sigma$	Case PW- 20%	Case PW-10%	Case PW+10%	Case PW+20%
$\Delta\Sigma$ 40	-1.3710	-0.6855	0.6855	1.3710
$\Delta\Sigma$ 41	-1.2437	-0.6219	0.6219	1.2437
$\Delta\Sigma$ 42	-0.0419	-0.0210	0.0210	0.0419
$\Delta\Sigma$ 43	0.0075	0.0038	-0.0038	-0.0075
$\Delta\Sigma$ 44	0.1874	0.0937	-0.0937	-0.1874

Source: The author

The same five cases were used to analyze the MSV of the system Jacobian matrix (4). Table 8 shows the five smallest MSV obtained when above variations of power are assumed in the Southern Brazilian Reduced System.

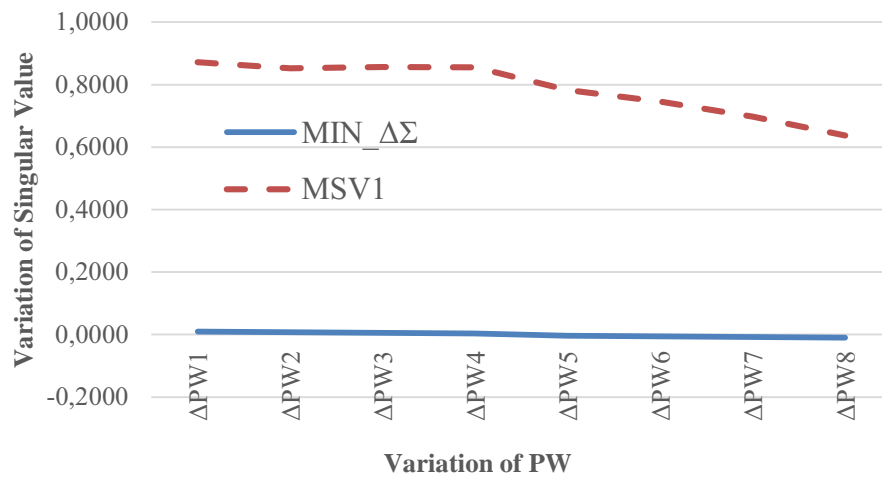
Table 7 - Smallest MSV of the Southern Brazilian Reduced System

MSV	20% Reduced	10% Reduced	Best Forecast	10% Increased	20% Increased
SV52	7.2954	7.2424	7.120834	6.9165	6.602381
SV53	5.6011	5.4918	5.349108	5.1678	4.94589
SV54	5.0900	5.0821	5.027065	4.9117	4.69765
SV55	2.4958	2.4839	2.448555	2.3857	2.286802
SV56	0.8523	8.5500	0.832783	0.7827	0.697624

Source: The author

Comparing Tables 7 and 8, again it is clear that the trend of MSV and $\Delta\Sigma$ remains the same. This can be concluded by examining the behavior of MSV and its trajectory to approach the point of collapse (zero). The trend can be verified by analyzing Figure 22. Apart from showing the same trend, the proposed method shows more sensitive variations.

This proves the accuracy of proposed method. It is also evident that the trend shows that a certain change in wind power output could cause voltage collapse when the transmission system is loaded more.

Figure 22 - MSV versus $\Delta\Sigma$ for the Southern Brazilian Reduced System

Source: The author

4.1.5 An Actual System

Finally, the study has been repeated for an actual system with 581 buses, which contains 145 conventional generators such as thermal and large hydro. Besides those generators, 437 wind generators were introduced into the system for the analysis. Locations of those wind generators were selected randomly. Because it is an actual system, to understand the effect of the variation of wind power on voltage stability, the standard deviations of wind power outputs were assumed. This system operates close to its voltage collapse point. Accordingly, it is impossible to assume higher wind uncertainties while considering large number of wind generators. Therefore, in order to apply the approach to the point of collapse, wind uncertainties given in Table 9 were assumed. Furthermore, Table 9 gives variations of $\Delta\Sigma$.

Table 8 - Variation of Smallest $\Delta\Sigma$ of 581- Bus System

$\Delta\Sigma$	Case PW- 20%	Case PW-10%	Case PW+10%	Case PW+20%
$\Delta\Sigma$ 576	-0.0045	-0.0023	0.0023	0.0045
$\Delta\Sigma$ 577	-0.0041	-0.0021	0.0021	0.0041
$\Delta\Sigma$ 578	-0.0007	-0.0004	0.0004	0.0007
$\Delta\Sigma$ 579	0.0019	0.0009	-0.0009	-0.0019
$\Delta\Sigma$ 580	0.0030	0.0015	-0.0015	-0.0030

Source: The author

A comparable analysis with the above wind generation cases was carried out with the system Jacobian matrix of the actual 581-bus system. The results of five smallest singular values are given in Table 10.

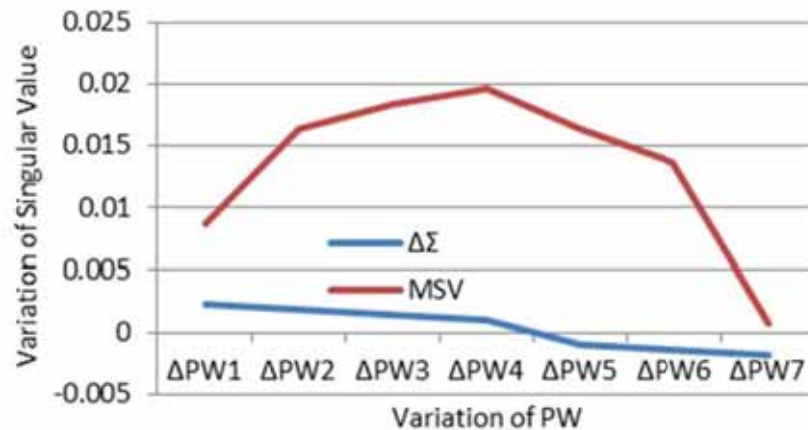
Table 9 - Smallest MSV of 581- Bus System

MSV	10% Reduced	5% Reduced	Best Forecast	5% Increase	10% Increase
SV576	0.6448	0.6429	0.6411	0.6395	0.6379
SV577	0.6196	0.6153	0.6105	0.6052	0.5994
SV578	0.5429	0.5429	0.5428	0.5427	0.5425
SV579	0.3170	0.3162	0.3154	0.3146	0.3137
SV580	0.0163	0.0158	0.0153	0.0148	0.0143

Source: The author

Figure 23 can better show the behavior of the 581-bus system. According to Figure, the system quickly approaches the point of collapse due to its inherent heavily loaded characteristic. While showing the same trend, the proposed method shows variations that are more sensitive.

Figure 23 - MSV versus $\Delta\Sigma$ for 581- Bus System



Source: The author

The important outcome, of these test cases, is that values of MSV determined by both the proposed method (that depends on one OPF solution and linear relations based upon Hessian of system power balance equations) and conventional method of repeated OPF solution and evaluation of system Jacobian always derive the same conclusion about influence of wind

uncertainty on voltage stability. The conventional method showed clear convergence problems when used for evaluation of a large system and heavily loaded. Considering the simplification of computation, the proposed method has a clear advantage compared to the conventional Jacobian technique using repeated OPF solutions. Furthermore, the proposed method establishes a linear relationship between wind power uncertainty and changes in minimum singular value of the system Jacobian, and thus, the system voltage stability.

Though the MSV do not necessarily provide the MW margin to voltage collapse, its change gives an indication about the change in system voltage stability margin. Hence, this method shows the effect of uncertainty of wind power forecast on the MSV of system Jacobian.

In addition, from the test cases it is clearly evident that wind power uncertainty affects voltage stability of transmission systems.

4.2 CHAPTER SUMMARY

This chapter presents the simulations for five test systems, including two real systems. The equations developed in Chapter 3 were implemented in Matlab Software and used to evaluate the uncertainty of wind generation on the stability of test systems. Result show evident superiority of the proposed technique over classical method in addition to the plus of building a linear relationship between wind power uncertainty and MSV.

5 CONCLUSION

5.1 RESEARCH CONTRIBUTIONS

This thesis addresses voltage stability challenges in the integration of wind energy into power systems. The main contributions of this research are listed below.

In this work, a linear relationship between uncertainty of wind power forecasts and variation of minimum singular values of the system Jacobian matrix is established using the Hessian matrix of the bus-wise power balance equations. Via this linear relationship, effect of uncertainty in wind power forecast on the system voltage stability can be effectively studied with a reduced computational burden.

The proposed method has an advantage. It establishes a direct link between the wind generation uncertainty and the minimum singular value. This problem is of significant interest to power system operators and national planning bureaus and is applicable to every country and market. Thus, instead of solving OPF repeatedly for determining minimum singular values for all possible cases of wind power generation, the proposed method allows to examine the direct effect of wind power forecast uncertainty on voltage stability.

Ward and Hale 6-bus, IEEE 57-bus, IEEE 118-bus systems and an actual system were used to verify the Hessian matrix-based relationship derived in this thesis. These studies yield good results on the Brazilian North-Northeast system as well as an actual 581 bus power system for the voltage stability analyses. An important conclusion is the fact that when the system is heavily loaded it will move quickly to the point of collapse. The conventional method showed clear convergence problems when used for evaluation of a large system and heavily loaded.

Another important conclusion is that minimum singular values of the proposed method shows the same trend as the minimum singular values of the full system Jacobian matrix method. This proves the accuracy of the proposed method. Furthermore, from the several case studies reported in this work, it is found that voltage stability issues can be expected in transmission systems with high wind penetrations.

5.2 FUTURE WORK

Another possible application of the proposed method is in case of other renewable sources with uncertainty such as solar power. It might be also possible to apply the theory developed in this work in hybrid systems.

This new methodology is original and can contribute greatly to the area; it can be also very useful in future developments.

REFERENCES

- ASSOCIAÇÃO BRASILEIRA DE ENERGIA EÓLICA- ABEÓLICA. **Dados do setor**. São Paulo: Portal ABEE,. 2014. Available: <<http://www.portalabeeolica.org.br/>>. Access: Oct, 10, 2014.
- ALVES, D. A.; LUIZ, C. P.; CASTRO, C. A.; COSTA, V. F. Alternative parameters for the continuation power flow method. **Electric Power Systems Research**, Lausanne, v. 1, n. 66, p. 105-113, 2003.
- AJJARAPU, V.; CHRISTY, C. The application of a locally parameterized continuation technique to the study of steady state voltage stability. In: ANNUAL NORTH AMERICAN POWER SYMPOSIUM, 21., 1989, New York. **Proceedings...** New York: IEEE, 1989. p. 161-167. 1989.
- ANDERSON, P. M.; FOUAD, A. A. **Power system control and stability**. New York: Institute of Electrical and Electronics Engineers, 1994. p. 464.
- AGÊNCIA NACIONAL DE ENERGIA ELÉTRICA- ANEEL. **Banco de dados de informações gerenciais- BIG**. Brasília: Banco de dados, 2014. Available:<<http://www.aneel.gov.br/>>. Access: Oct. 10 2014.
- ARYA, L.; CHOUBE, S. A.; SHRIVASTAVA, M. Technique for voltage stability assessment using newly developed line voltage stability index. **Energy Conversion and Management**, Oxford, v. 49, n. 2, p. 267-275, 2008.
- BEN-KILANI, K.; ELLEUCH, M. Structural analysis of voltage stability in power systems integrating wind power. **IEEE Transactions Power Systems**, New York, v. 28, n. 4, p. 3785-3794, 2013.
- BU, S. Q.; DU, W.; WANG, H.F.; CHEN, Z.; XIAO, L. Y.; LI, H.F. Probabilistic analysis of small-signal stability of large-scale power systems as affected by penetration of wind generation. **IEEE Transactions Power Systems**, New York, v. 27, n. 2, p. 762-770, May 2012.
- BURCHETT, R. C.; HEYDT, G. T. Probabilistic methods for power system dynamic stability studies. **IEEE Transactions Power Apparatus and Systems**, New York, v. PAS-97, n. 3, p. 695-702, May 1978.

CANIZARES, C. A.; ALVARADO, F. L. Point of collapse and continuation methods for large AC/DC systems. **IEEE Transactions on Power Systems**, New York, v. 8, n. 1, p. 1-8, Feb. 1993.

CHEN, K.; HUSSEIN, A.; WAN, H. B. On a class of new and practical performance indexes for approximation of fold bifurcations of nonlinear power flow equations. **Journal of Computational and Applied Mathematics**, Antwerpen, v. 140, n. 1-2, p. 119-141, 2002.

CHIANG, H. D. **CPFLOW for power tracer and voltage monitoring**. Ithaca: Cornell University/Power System Engineering Research Centre, 2002. (Final report, Power System Engineering Research Centre, 2002). Available: <http://www.pserc.wisc.edu/ecow/get/publicatio/2001public/chiang_report.pdf>. Access: July 30, 2014.

DE SOUZA, A. C.Z.; CANIZARES, C. A; QUINTANA, V. H. New techniques to speed up voltage collapse computations using tangent vectors. **IEEE Transactions on Power Systems**, New York, v. 12, n. 3, p. 1380-1387, Aug. 1997.

ELA, E.; MILLIGAN, M.; PARSONS, B.; LEW D.; CORBUS, D. The evolution of wind power integration studies: past, present, and future. In: IEEE POWER ENGINEERING SOCIETY GENERALMEETING, 2009, Denver. **Proceedings...** Denver: PES-IEEE, 2009. p. 1-8.

GLOBAL WIND ENERGY COUNCIL- GWEC. **Global wind report annual market update**. [S.l.: s.n.], 2014. Available: <<http://www.gwec.net>>. Access: Oct 10 2014.

GRIGG, C. Power system test case archive. In: IEEE WINTER POWER MEETING, 1996, Washington. **Meeting...** Washington; [s.n.], 1996. Available: <<http://www.ee.washington.edu/research/ptca/>>. Access: July 10 2014.

GUCKENHEIMER, J.; HOLMES, P. **Nonlinear oscillations, dynamical systems, and bifurcations of vector fields**. New York: Springer Verlag, 1997. (Applied Mathematical Sciences, 42).

HODGE, B.; MILLIGAN, M. Wind power forecasting error distributions over multiple timescales. IEEE POWER ENGINEERING SOCIETY GENERALMEETING, 2009, Calgary. **Proceedings...** Calgary: PES-IEEE, 2011.

INTERNATIONAL ENERGY AGENCY- IEA. **World energy outlook**. [S.l.: s.n.], 2012. Available: <<http://www.worldenergyoutlook.org/publications/weo-2014/>>.Access: Oct. 10 2014.

JIA, Z. A. Contingency ranking for on-line voltage stability assessment. **IEEE Transactions on Power System**, New York, v. 15, n. 3, p. 1093-1097, 2000.

- KUNDUR, P. **Power system stability and control**. New York: McGraw-Hill, 1994. 1176 p. (Electric Power Research Institute).
- LEONARDI, B.; AJJARAPU, V. Development of multilinear regression models for online voltage stability margin estimation. **IEEE Transactions on Power Systems**, New York, v. 26, n. 1, p. 374-383, Feb. 2011.
- LOF, P. A.; SMED, T.; ANDERSON, G. ; HILL, D. J. Fast calculation of a voltage stability index. **IEEE Transactions on Power Systems**, New York, v. 7, p. 54-64, 1992.
- LOUIE, H. Evaluation of probabilistic models of wind plant power output characteristics. In: INTERNATIONAL CONFERENCE ON PROBABILISTIC METHODS APPLIED TO POWER SYSTEMS-PMAPS, 1., 2010, Singapore. **Conference...** Singapore: IEEE, 2010. p. 442-447.
- MINUSSI, C. R. **Controle de segurança dinâmica em sistemas de energia elétrica**. 1990. Tese (Doutorado) – Faculdade de Engenharia Elétrica, Universidade Federal de Santa Catarina, Florianópolis, 1990.
- MORISON G. K.; GAO, B.; KUNDUR, P. Voltage stability analysis using static and dynamic approaches. **IEEE Transactions Power Systems**, New York, v. 8, n. 3, p. 1159–1171, Aug. 1993.
- NAN, H. K.; KIM, Y. K.; SHIM, K. A.; LEE, K. Y. A new eigen-sensibility theory of augmented matrix and its applications to power systems stability analysis. **IEEE Transaction on Power Systems**, New York, v. 15, n. 1, p. 363-369, 2000.
- ORTEGA-VAZQUEZ, M.; KIRSCHEN D. Assessing the impact of wind power generation on operating costs. **IEEE Trans. Smart Grid**, New York, v. 1, n. 3, p. 295–301, 2010.
- PAI, M. A. **Power system stability: analysis by direct of Lyapunov**. Amsterdam: NorthHolland, 1981. 251 p.
- PATERNI, P.; VITET, S.; BENA, M; YOKOYAMA, A. Optimal location of phase shifters in the French network by genetic algorithm. **IEEE Transactions Power System**, New York, v. 14, n. 1, p. 37–42, Feb. 1999.
- PAVELLA, M.; MURTHY, P. G. **Transient stability of power systems: theory and practice**. Chichester: John Wiley & Sons, 1994. 403 p.
- PETEAN-PINA, A.; ARAUJO, P. B. de. Comparison of factsstatcom models for damping oscillations in power system due to small perturbations. In: TRANSMISSION AND DISTRIBUTION CONFERENCE AND EXPOSITION: LATIN AMERICA. 5., 2010, São Paulo. **Conference...** São Paulo: IEEE/PES, 2001. v. 1, p. 465-471.

RAVE K. **Wind is a global power source global wind energy council**. Sidney: [s.n.]. 2013. Available: <http://www.carbonfairgo.com.au/forum_post.php?i=46>. Access: July 10 2013.

RESTREPO J.; GALIANA, F. Assessing the yearly impact of wind power through a new hybrid deterministic/stochastic unit commitment. **IEEE Transactions Power Systems**, New York: v. 26, n. 1, p. 401-410, Feb. 2011.

ROMERO, R.; MANTOVANI, J. R. S. Introdução a metaheurísticas. In: CONGRESSO TEMÁTICO DE DINÂMICA E CONTROLE DA SBMAC, 3., 2004, Ilha Solteira. **Anais...** Ilha solteira: SBMAC, 2004. p. 1-10.

SAUER, P. W.; PAI, M. A. Power system steady-state stability and the load flow jacobian. **IEEE Transactions on Power Systems**, New York, v. PWRS-5, n. 4, p. 1374-1383, 1990.

SHORTT, A.; KIVILUOMA, J.; O'MALLEY, M. Accommodating variability in generation planning. **IEEE Transactions Power Systems**, New York, v. 28, n.1, p.158-169, Feb. 2013.

SINHA, A. A.; HAZARIKA, D. A comparative study of voltage stability indices in a powersystem. **Electrical Power & Energy Systems**, Guildford, v. 1, n.22, p. 589-596, 2000.

SMITH, J. C.; MILLIGAN, M. R.; DEMEO, E. A.; PARSONS, B. Utility wind integration and operating impact state of the art. **IEEE Transactions Power Systems**, New York, v. 22, n .3, p. 900-908, Aug. 2007.

SMITH, J. C.; AHLSTROM, M. L.; ZAVADIL, R. M.; SADJADPOUR, A.; PHILBRICK, C. R. The role of wind forecasting in utility system operation. In: POWER & ENERGY SOCIETY GENERAL MEETING- PES, 2009, Calgary. **Meeting...** [S.l.], IEEE/PES, 2009. p. 1-5.

SMON, I; VERBIC, G.; GUBINA, F. Local voltage-stability index using tellegen's theorem. **IEEE Transactions Power Systems**, New York, v. 21, n. 3, p. 1267-1275, Aug. 2006.

TIRANUCHIT, A.; THOMAS, R. J. A posturing strategy against voltage instabilities in electric power systems. **IEEE Transactions Power Systems**, New York, v. 3, n. 1, p. 87-93, Feb. 1988.

UMMELS, B.; GIBESCU, M.; PELGRUM, E.; KLING, W.; BRAND A. Impacts of wind power on thermal generation unit commitment and dispatch. **IEEE Trans. Energy Convers**, New York, v. 22, n. 1, p. 44–51, Mar. 2007.

VAN CUTSEM, T.; VOURNAS, C. **Voltage stability of electric power systems**. London: Kluwer Academic Publishers, 1998. 462 p.

VAN CUTSEM, T. Voltage instability: phenomena, countermeasures, and analysis methods. **Proceedings of the IEEE**, New York, v. 88, n. 2, p. 208–227, 2000.

VENKATESH, B.; ROST, A.; LIUCHEN, C. Dynamic voltage collapse index— wind generator application, power delivery. **IEEE Transactions Power Systems**, New York, v. 22, n. 1, p. 90-94, Jan. 2007.

VERBIC, G.; GUBINA, F. Fast voltage-collapse line-protection algorithm based on local phasors. **Proceeding of IEEE, Gen. Transm. Distrib.**, New York, v. 150, n. 4, p. 482–486., July. 2003.

VERBIC, G.; GUBINA, F. A new concept of voltage-collapse protection based on local phasors. **IEEE Transactions Power Systems**, New York, v. 19, n. 2, p. 576–581, Apr. 2004.

VOURNAS, C.D. Voltage stability and controllability indices for multimachine power systems **IEEE Transactions Power Systems**, New York, v. 10, n. 3, p. 1183-1194, Aug. 1995.

VU, K.; LIU, C. C.; TAYLOR, C. W.; JIMMA, K. Voltage instability: mechanisms and control strategies. **Proceeding of the IEEE**, New York, v. 83, n. 11, p. 1442-1455, 1995.

ZAMBRONI, A. C. S. Discussions on some voltage collapse indices. **Electric Power Systems Research**, Lausanne, v. 53, n. 1, p. 53-58, 2000.

ZHANG, N.; KANG, C.; XIA, Q.; LIANG, L. Modeling conditional forecast error for wind power in generation scheduling. **IEEE Transactions Power Systems**, New York, v. 29, n. 3, p. 1316-1324, May 2014.

APPENDIX A – DATA OF SYSTEM

IEEE- 6 Bus System Data

MVA Base=100 MVA

System Frequency = 50 Hz

Bus Nominal Voltage =11KV

Bus Maximum Voltage = 11.5 KV

Bus Minimum Voltage = 10.4 KV

Table A-I: Load Data

Bus	Real Power, Mw	Reactive Power, MVAR
At Bus 2	20	10
At Bus 5	40	15
At Bus 6	30	10

Table A-II: Line Data

Line No.	Bus Code p-q	Positive Sequence Resistance, p.u	Positive Sequence Reactance, p.u
1	1-2	0.05	0.20
2	2-3	0.10	0.50
3	3-4	0.20	0.80
4	4-5	0.10	0.30
5	5-6	0.20	0.40
6	6-1	0.10	0.15
7	2-5	0.20	0.50

Table A-III: Generator Data

Generator No.	P+j Q p.u.	V p.u.	MVA	Bus Type
G1	0+j0	1.00	100	Slack
G2	0.1+j0.05	1.041	15	PV
G3	0.30+j0.2	1.0190	40	PV
G4	0.2+j0.1	1.071	30	PV

The IEEE 57 bus Power System is used in the thesis for different simulations conducted in Chapter 4. The bus data and transmission line data are given at 100MVA in Table A-IV and Table A-V, respectively.

Table A-IV: Bus data for the IEEE57 bus Power System (inp.u.)

Bus No.	$P_{G,i}$	$P_{D,i}$	$Q_{D,i}$	V_i	V_{max}	V_{min}
1	4.7926	0.5500	0.1700	1.0400	1.10	0.90
2	0.0000	0.0300	0.8800	1.0100	1.10	0.90
3	0.4000	0.4100	0.2100	0.9850	1.10	0.90
4	0.0000	0.0000	0.0000	0.9783	1.06	0.94
5	0.0000	0.1300	0.0400	0.9757	1.06	0.94
6	0.0000	0.7500	0.0200	0.9800	1.10	0.90
7	0.0000	0.0000	0.0000	0.9819	1.06	0.94
8	4.5000	1.5000	0.2200	1.0050	1.10	0.90
9	0.0000	1.2100	0.2600	0.9800	1.06	0.94
10	0.0000	0.0500	0.0200	0.9857	1.10	0.90
11	0.0000	0.0000	0.0000	0.9732	1.06	0.94
12	3.1000	3.7700	0.2400	1.0150	1.10	0.90
13	0.0000	0.1800	0.0230	0.9779	1.06	0.94
14	0.0000	0.1050	0.0530	0.9688	1.06	0.94
15	0.0000	0.2200	0.0500	0.9871	1.06	0.94
16	0.0000	0.4300	0.0300	1.0133	1.06	0.94
17	0.0000	0.4200	0.0800	1.0174	1.06	0.94
18	0.0000	0.2720	0.0980	0.9751	1.06	0.94
19	0.0000	0.0330	0.0060	0.9515	1.06	0.94
20	0.0000	0.0230	0.0100	0.9497	1.06	0.94
21	0.0000	0.0000	0.0000	1.0004	1.06	0.94
22	0.0000	0.0000	0.0000	1.0029	1.06	0.94
23	0.0000	0.0630	0.0210	1.0010	1.06	0.94
24	0.0000	0.0000	0.0000	0.9842	1.06	0.94
25	0.0000	0.0630	0.0320	0.9378	1.06	0.94
26	0.0000	0.0000	0.0000	0.9453	1.06	0.94
27	0.0000	0.0930	0.0050	0.9727	1.06	0.94
28	0.0000	0.0460	0.0230	0.9896	1.06	0.94
29	0.0000	0.1700	0.0260	1.0043	1.06	0.94
30	0.0000	0.0360	0.0180	0.9201	1.06	0.94
31	0.0000	0.0580	0.0290	0.8999	1.06	0.94
32	0.0000	0.0160	0.0080	0.9259	1.06	0.94
33	0.0000	0.0380	0.0190	0.9236	1.06	0.94
34	0.0000	0.0000	0.0000	0.9491	1.06	0.94
35	0.0000	0.0600	0.0300	0.9575	1.06	0.94
36	0.0000	0.0000	0.0000	0.9682	1.06	0.94
37	0.0000	0.0000	0.0000	0.9778	1.06	0.94
38	0.0000	0.1400	0.0700	1.0071	1.06	0.94
39	0.0000	0.0000	0.0000	0.9758	1.06	0.94
40	0.0000	0.0000	0.0000	0.9653	1.06	0.94
41	0.0000	0.0630	0.0300	0.9938	1.06	0.94
42	0.0000	0.0710	0.0440	0.9631	1.06	0.94
43	0.0000	0.0200	0.0100	1.0083	1.06	0.94
44	0.0000	0.1200	0.0180	1.0121	1.06	0.94
45	0.0000	0.0000	0.0000	1.0334	1.06	0.94
46	0.0000	0.0000	0.0000	1.0570	1.06	0.94
47	0.0000	0.2970	0.1160	1.0292	1.06	0.94
48	0.0000	0.0000	0.0000	1.0229	1.06	0.94
49	0.0000	0.1800	0.0850	1.0328	1.06	0.94
50	0.0000	0.2100	0.1050	1.0207	1.06	0.94
51	0.0000	0.1800	0.0530	1.0513	1.06	0.94
52	0.0000	0.0490	0.0220	0.9676	1.06	0.94

53	0.0000	0.2000	0.1000	0.9546	1.06	0.94
54	0.0000	0.0410	0.0140	0.9866	1.06	0.94
55	0.0000	0.0680	0.0340	1.0276	1.06	0.94
56	0.0000	0.0760	0.0220	0.9641	1.06	0.94
57	0.0000	0.0670	0.0200	0.9600	1.06	0.94

Table A-V: Transmission line data for the IEEE57 bus Power System (inp.u.)

Line No.	From Bus No.	To Bus No.	R	X	Bch(Full)	Max Line
1	1	2	0.0083	0.0280	0.1290	99.00
2	2	3	0.0298	0.0850	0.0818	99.00
3	3	4	0.0112	0.0366	0.0380	99.00
4	4	5	0.0625	0.1320	0.0258	99.00
5	4	6	0.0430	0.1480	0.0348	99.00
6	6	7	0.0200	0.1020	0.0276	99.00
7	6	8	0.0339	0.1730	0.0470	99.00
8	8	9	0.0099	0.0505	0.0548	99.00
9	9	10	0.0369	0.1679	0.0440	99.00
10	9	11	0.0258	0.0848	0.0218	99.00
11	9	12	0.0648	0.2950	0.0772	99.00
12	9	13	0.0481	0.1580	0.0406	99.00
13	13	14	0.0132	0.0434	0.0110	99.00
14	13	15	0.0269	0.0869	0.0230	99.00
15	1	15	0.0178	0.0910	0.0988	99.00
16	1	16	0.0454	0.2060	0.0546	99.00
17	1	17	0.0238	0.1080	0.0286	99.00
18	3	15	0.0162	0.0530	0.0544	99.00
19	4	18	0.0000	0.5550	0.0000	99.00
20	4	18	0.0000	0.4300	0.0000	99.00
21	5	6	0.0302	0.0641	0.0124	99.00
22	7	8	0.0139	0.0712	0.0194	99.00
23	10	12	0.0277	0.1262	0.0328	99.00
24	11	13	0.0223	0.0732	0.0188	99.00
25	12	13	0.0178	0.0580	0.0604	99.00
26	12	16	0.0180	0.0813	0.0216	99.00
27	12	17	0.0397	0.1790	0.0476	99.00
28	14	15	0.0171	0.0547	0.0148	99.00
29	18	19	0.4610	0.6850	0.0000	99.00
30	19	20	0.2830	0.4340	0.0000	99.00
31	21	20	0.0000	0.7767	0.0000	99.00
32	21	22	0.0736	0.1170	0.0000	99.00
33	22	23	0.0099	0.0152	0.0000	99.00
34	23	24	0.1660	0.2560	0.0084	99.00
35	24	25	0.0000	1.1820	0.0000	99.00
36	24	25	0.0000	1.2300	0.0000	99.00
37	24	26	0.0000	0.0473	0.0000	99.00
38	26	27	0.1650	0.2540	0.0000	99.00
39	27	28	0.0618	0.0954	0.0000	99.00
40	28	29	0.0418	0.0587	0.0000	99.00
41	7	29	0.0000	0.0648	0.0000	99.00
42	25	30	0.1350	0.2020	0.0000	99.00
43	30	31	0.3260	0.4970	0.0000	99.00
44	31	32	0.5070	0.7550	0.0000	99.00
45	32	33	0.0392	0.0360	0.0000	99.00
46	34	32	0.0000	0.9530	0.0000	99.00
47	34	35	0.0520	0.0780	0.0032	99.00

48	35	36	0.0430	0.0537	0.0016	99.00
49	36	37	0.0290	0.0366	0.0000	99.00
50	37	38	0.0651	0.1009	0.0020	99.00
51	37	39	0.0239	0.0379	0.0000	99.00
52	36	40	0.0300	0.0466	0.0000	99.00
53	22	38	0.0192	0.0295	0.0000	99.00
54	11	41	0.0000	0.7490	0.0000	99.00
55	41	42	0.2070	0.3520	0.0000	99.00
56	41	43	0.0000	0.4120	0.0000	99.00
57	38	44	0.0289	0.0585	0.0020	99.00
58	15	45	0.0000	0.1042	0.0000	99.00
59	14	46	0.0000	0.0735	0.0000	99.00
60	46	47	0.0230	0.0680	0.0032	99.00
61	47	48	0.0182	0.0233	0.0000	99.00
62	48	49	0.0834	0.1290	0.0048	99.00
63	49	50	0.0801	0.1280	0.0000	99.00
64	50	51	0.1386	0.2200	0.0000	99.00
65	10	51	0.0000	0.0712	0.0000	99.00
66	13	49	0.0000	0.1910	0.0000	99.00
67	29	52	0.1442	0.1870	0.0000	99.00
68	52	53	0.0762	0.0984	0.0000	99.00
69	53	54	0.1878	0.2320	0.0000	99.00
70	54	55	0.1732	0.2265	0.0000	99.00
71	11	43	0.0000	0.1530	0.0000	99.00
72	44	45	0.0624	0.1242	0.0040	99.00
73	40	56	0.0000	1.1950	0.0000	99.00
74	56	41	0.5530	0.5490	0.0000	99.00
75	56	42	0.2125	0.3540	0.0000	99.00
76	39	57	0.0000	1.3550	0.0000	99.00
77	57	56	0.1740	0.2600	0.0000	99.00
78	38	49	0.1150	0.1770	0.0030	99.00
79	38	48	0.0312	0.0482	0.0000	99.00
80	9	55	0.0000	0.1205	0.0000	99.00

The IEEE 118 bus Power System is used in the thesis for different simulations conducted in Chapter 4. The bus data and transmission line data are given at 100MVA in Table A-VI and Table A-VII, respectively.

Table A-VI Line Data of the IEEE118-Bus System

Line	From Bus	To Bus	R (p.u.)	X (p.u.)	Line	From Bus	To Bus	R (p.u.)	X (p.u.)
1	1	2	0.0303	0.0999	47	35	37	0.011	0.0497
2	1	3	0.0129	0.0424	48	33	37	0.0415	0.142
3	4	5	0.0018	0.008	49	34	36	0.0087	0.0268
4	3	5	0.0241	0.108	50	34	37	0.0026	0.0094
5	5	6	0.0119	0.054	51	38	37	o	0.0375
6	6	7	0.0046	0.0208	52	37	39	0.0321	0.106
7	8	9	0.0024	0.0305	53	37	40	0.0593	0.168
8	8	5	o	0.0267	54	30	38	0.0046	0.054
9	9	10	0.0026	0.0322	55	39	40	0.0184	0.0605
10	4	11	0.0209	0.0688	56	40	41	0.0145	0.0487
11	5	11	0.0203	0.0682	57	40	42	0.0555	0.183
12	11	12	0.006	0.0196	58	41	42	0.041	0.135
13	2	12	0.0187	0.0616	59	43	44	0.0608	0.2454
14	3	12	0.0484	0.16	60	34	43	0.0413	0.1681
15	7	12	0.0086	0.034	61	44	45	0.0224	0.0901
16	11	13	0.0223	0.0731	62	45	46	0.04	0.1356
17	12	14	0.0215	0.0707	63	46	47	0.038	0.127
18	13	15	0.0744	0.2444	64	46	48	0.0601	0.189
19	14	15	0.0595	0.195	65	47	49	0.0191	0.0625
20	12	16	0.0212	0.0834	66	42	49	0.0715	0.323
21	15	17	0.0132	0.0437	67	42	49	0.0715	0.323
22	16	17	0.0454	0.1801	68	45	49	0.0684	0.186
23	17	18	0.0123	0.0505	69	48	49	0.0179	0.0505
24	18	19	0.0112	0.0493	70	49	50	0.0267	0.0752
25	19	20	0.0252	0.117	71	49	51	0.0486	0.137
26	15	19	0.012	0.0394	72	51	52	0.0203	0.0588
27	20	21	0.0183	0.0849	73	52	53	0.0405	0.1635
28	21	22	0.0209	0.097	74	53	54	0.0263	0.122
29	22	23	0.0342	0.159	75	49	54	0.073	0.289
30	23	24	0.0135	0.0492	76	49	54	0.0869	0.291
31	23	25	0.0156	0.08	77	54	55	0.0169	0.0707
32	26	25	o	0.0382	78	54	56	0.0027	0.0095
33	25	27	0.0318	0.163	79	55	56	0.0049	0.0151
34	27	28	0.0191	0.0855	80	56	57	0.0343	0.0966
35	28	29	0.0237	0.0943	81	50	57	0.0474	0.134
36	30	17	o	0.0388	82	56	58	0.0343	0.0966
37	8	30	0.0043	0.0504	83	51	58	0.0255	0.0719
38	26	30	0.008	0.086	84	54	59	0.0503	0.2293
39	17	31	0.0474	0.1563	85	56	59	0.0825	0.251
40	29	31	0.0108	0.0331	86	56	59	0.0803	0.239
41	23	32	0.0317	0.1153	87	55	59	0.0474	0.2158
42	31	32	0.0298	0.0985	88	59	60	0.0317	0.145
43	27	32	0.0229	0.0755	89	59	61	0.0328	0.15
44	15	33	0.038	0.1244	90	60	61	0.0026	0.0135
45	19	34	0.0752	0.247	91	60	62	0.0123	0.0561
46	35	36	0.0022	0.0102	92	61	62	0.0082	0.0376

Line	From Bus	To Bus	R (p.u.)	X (p.u.)	Line	From Bus	To Bus	R (p.u.)	X (p.u.)
93	63	59	o	0.0386	140	90	91	0.0254	0.0836
94	63	64	0.0017	0.02	141	89	92	0.0099	0.0505
95	64	61	o	0.0268	142	89	92	0.0393	0.1581
96	38	65	0.009	0.0986	143	91	92	0.0387	0.1272
97	64	65	0.0027	0.0302	144	92	93	0.0258	0.0848
98	49	66	0.018	0.0919	145	92	94	0.0481	0.158
99	49	66	0.018	0.0919	146	93	94	0.0223	0.0732
100	62	66	0.0482	0.218	147	94	95	0.0132	0.0434
101	62	67	0.0258	0.117	148	80	96	0.0356	0.182
102	65	66	o	0.037	149	82	96	0.0162	0.053
103	66	67	0.0224	0.1015	150	94	96	0.0269	0.0869
104	65	68	0.0014	0.016	151	80	97	0.0183	0.0934
105	47	69	0.0844	0.2778	152	80	98	0.0238	0.108
106	49	69	0.0985	0.324	153	80	99	0.0454	0.206
107	68	69	o	0.037	154	92	100	0.0648	0.295
108	69	70	0.03	0.127	155	94	100	0.0178	0.058
109	24	70	0.0022	0.4115	156	95	96	0.0171	0.0547
110	70	71	0.0088	0.0355	157	96	97	0.0173	0.0885
111	24	72	0.0488	0.196	158	98	100	0.0397	0.179
112	71	72	0.0446	0.18	159	99	100	0.018	0.0813
113	71	73	0.0087	0.0454	160	100	101	0.0277	0.1262
114	70	74	0.0401	0.1323	161	92	102	0.0123	0.0559
115	70	75	0.0428	0.141	162	101	102	0.0246	0.112
116	69	75	0.0405	0.122	163	100	103	0.016	0.0525
117	74	75	0.0123	0.0406	164	100	104	0.0451	0.204
118	76	77	0.0444	0.148	165	103	104	0.0466	0.1584
119	69	77	0.0309	0.101	166	103	105	0.0535	0.1625
120	75	77	0.0601	0.1999	167	100	106	0.0605	0.229
121	77	78	0.0038	0.0124	168	104	105	0.0099	0.0378
122	78	79	0.0055	0.0244	169	105	106	0.014	0.0547
123	77	80	0.017	0.0485	170	105	107	0.053	0.183
124	77	80	0.0294	0.105	171	105	108	0.0261	0.0703
125	79	80	0.0156	0.0704	172	106	107	0.053	0.183
126	68	81	0.0018	0.0202	173	108	109	0.0105	0.0288
127	81	80	0	0.037	174	103	110	0.0391	0.1813
128	77	82	0.0298	0.0853	175	109	110	0.0278	0.0762
129	82	83	0.0112	0.0366	176	110	111	0.022	0.0755
130	83	84	0.0625	0.132	177	110	112	0.0247	0.064
131	83	85	0.043	0.148	178	17	113	0.0091	0.0301
132	84	85	0.0302	0.0641	179	32	113	0.0615	0.203
133	85	86	0.035	0.123	180	32	114	0.0135	0.0612
134	86	87	0.0283	0.2074	181	27	115	0.0164	0.0741
135	85	88	0.02	0.102	182	114	115	0.0023	0.0104
136	85	89	0.0239	0.173	183	68	116	0.0003	0.0041
137	88	89	0.0139	0.0712	184	12	117	0.0329	0.14
138	89	90	0.0518	0.188	185	75	118	0.0145	0.0481
139	89	90	0.0238	0.0997	186	76	118	0.0164	0.0544

Table A-VII Bus Load and Injection Data of the IEEE118-Bus System

Bus	Type	pd	Qd	Pg	Qg	Bus	Type	pd	Qd	Pg	Qg
1	2	51	27	0	0	60	0	78	3	0	0
2	0	20	9	0	0	61	2	0	0	160	0
3	0	39	10	0	0	62	2	77	14	0	0
4	2	30	12	-9	0	63	0	0	0	0	0
5	0	0	0	0	0	64	0	0	0	0	0
6	2	52	22	0	0	65	2	0	0	391	0
7	0	19	2	0	0	66	2	39	18	392	0
8	2	0	0	-28	0	67	0	28	7	0	0
9	0	0	0	0	0	68	0	0	0	0	0
10	2	0	0	450	0	69	3	0	0	516.4	0
11	0	70	23	0	0	70	2	66	20	0	0
12	2	47	10	85	0	71	0	0	0	0	0
13	0	34	16	0	0	72	2	0	0	-12	0
14	0	14	1	0	0	73	2	0	0	-6	0
15	2	90	30	0	0	74	2	68	27	0	0
16	0	25	10	0	0	75	0	47	11	0	0
17	0	11	3	0	0	76	2	68	36	0	0
18	2	60	34	0	0	77	2	61	28	0	0
19	2	45	25	0	0	78	0	71	26	0	0
20	0	18	3	0	0	79	0	39	32	0	0
21	0	14	8	0	0	80	2	130	26	477	0
22	0	10	5	0	0	81	0	0	0	0	0
23	0	7	3	0	0	82	0	54	27	0	0
24	2	0	0	-13	0	83	0	20	10	0	0
25	2	0	0	220	0	84	0	11	7	0	0
26	2	0	0	314	0	85	2	24	15	0	0
27	2	62	13	-9	0	86	0	21	10	0	0
28	0	17	7	0	0	87	2	0	0	4	0
29	0	24	4	0	0	88	0	48	10	0	0
30	0	0	0	0	0	89	2	0	0	607	0
31	2	43	27	7	0	90	2	78	42	-85	0
32	2	59	23	0	0	91	2	0	0	-10	0
33	0	23	9	0	0	92	2	65	10	0	0
34	2	59	26	0	0	93	0	12	7	0	0
35	0	33	9	0	0	94	0	30	16	0	0
36	2	31	17	0	0	95	0	42	31	0	0
37	0	0	0	0	0	96	0	38	15	0	0
38	0	0	0	0	0	97	0	15	9	0	0
39	0	27	11	0	0	98	0	34	8	0	0
40	2	20	23	-46	0	99	2	0	0	-42	0
41	0	37	10	0	0	100	2	37	18	252	0
42	2	37	23	-59	0	101	0	22	15	0	0
43	0	18	7	0	0	102	0	5	3	0	0
44	0	16	8	0	0	103	2	23	16	40	0
45	0	53	22	0	0	104	2	38	25	0	0
46	2	28	10	19	0	105	2	31	26	0	0
47	0	34	0	0	0	106	0	43	16	0	0
48	0	20	11	0	0	107	2	28	12	-22	0
49	2	87	30	204	0	108	0	2	1	0	0
50	0	17	4	0	0	109	0	8	3	0	0
51	0	17	8	0	0	110	2	39	30	0	0
52	0	18	5	0	0	111	2	0	0	36	0
53	0	23	11	0	0	112	2	25	13	-43	0
54	2	113	32	48	0	113	2	0	0	-6	0
55	2	63	22	0	0	114	0	8	3	0	0
56	2	84	18	0	0	115	0	22	7	0	0
57	0	12	3	0	0	116	2	0	0	-184	0
58	0	12	3	0	0	117	0	20	8	0	0
59	2	277	113	155	0	118	0	33	15	0	0

The Southern Brazilian Reduced System is used in the thesis for different simulations conducted in Chapter 4. The bus data and transmission line data are given at 100MVA in Table A-VIII and Table A-IX, respectively.

Table A-VIII Line Data of the Southern Brazilian Reduced System

From Bus	To Bus	R (pu)	X (pu)	B (pu)
11	12	0,0007	0,0145	1,5672
11	12	0,0007	0,0145	1,5672
11	25	0,0018	0,0227	2,1230
11	33	0,0014	0,0204	2,2869
12	42	0	0,0063	0
1	29	0	0,0135	0
13	14	0,0386	0,1985	0,3425
13	35	0,0096	0,0491	0,0861
13	45	0,0033	0,0167	0,3019
14	15	0,0463	0,3378	0,3917
14	15	0,0463	0,3378	0,3917
14	37	0,0177	0,0910	0,1510
14	37	0,0177	0,0910	0,1510
14	37	0,0177	0,0910	0,1510
2	15	0	0,0460	0
15	16	0,0163	0,0835	0,1411
15	16	0,0163	0,0835	0,1411
15	39	0,0250	0,1648	0,4581
16	17	0,0163	0,0835	0,1445
16	18	0,0316	0,1621	0,2746
17	18	0,0153	0,0861	0,1328
3	18	0	0,0114	0
18	19	0,0306	0,1523	0,2620
18	44	0,0344	0,1760	0,3061
18	44	0,0344	0,1760	0,3061
19	20	0,0245	0,1256	0,1981
19	25	0	0,0300	0
20	21	0,0088	0,0415	0,5009
21	22	0,0182	0,0935	0,1602
21	22	0,0182	0,0935	0,1602
21	26	0	0,0062	0
22	23	0,0154	0,0776	0,1386
22	23	0,0154	0,0776	0,1386
23	24	0,0216	0,1105	0,1872
23	24	0,0216	0,1105	0,1872
23	28	0	0,0062	0
24	35	0,0180	0,0920	0,1556
24	35	0,0180	0,0920	0,1556
4	25	0	0,0067	0
25	26	0,0019	0,0280	3,1526
25	27	0,0019	0,0274	3,0741
25	29	0,0014	0,0195	2,2505
25	36	0,0005	0,0070	0,7857
26	27	0,0005	0,0069	0,7728
26	28	0,0012	0,0175	2,0160
29	30	0,0021	0,0300	3,5289
30	38	0	0,0062	0
31	32	0,0022	0,0300	3,6137

31	40	0	0,0062	0
32	33	0,0014	0,0195	2,2441
5	33	0	0,0114	0
33	36	0,0005	0,0070	0,7856
6	34	0	0,0871	0
34	35	0	0,0590	0
7	35	0	0,0701	0
8	35	0	0,0450	0
35	45	0,0129	0,0657	0,1155
10	36	0	0,0068	0
37	38	0,0021	0,0107	0,0208
37	38	0,0021	0,0107	0,0208
37	38	0,0021	0,0107	0,0208
37	40	0,0184	0,0949	0
37	40	0,0184	0,0949	0
37	40	0,0184	0,0949	0
9	39	0	0,0236	0
39	40	0,0202	0,1129	0,1993
41	42	0,0106	0,0596	0,0951
41	42	0,0106	0,0596	0,0951
41	43	0,0110	0,1184	0,2081
41	44	0,0229	0,1174	0,2087
42	43	0,0172	0,0884	0,1446
42	43	0,0172	0,0884	0,1446
43	44	0,0181	0,0929	0,1671

Table A-VII Bus Load and Injection Data of the Southern Brazilian Reduced System

Bus	V (pu)	Ang. (graus)	P _G (MW)	Q _G (MVar)	P _L (MW)	Q _L (MVar)
1	1,0000	-7,3485	650	53,49	-	-
2	1,0000	-14,9124	215	50,30	-	-
3	1,0000	2,9208	895	134,66	-	-
4	1,0000	0	1541,35	43,67	-	-
5	1,0000	7,2644	1325	55,68	-	-
6	1,0000	-26,2560	90	44,12	-	-
7	1,0000	-24,6624	120	51,29	-	-
8	1,0000	-23,2146	241	85,31	-	-
9	1,0000	-15,6540	460	134,08	-	-
10	1,0000	2,8229	1100	-20,01	-	-
11	0,9953	-7,3322	-	-	-	-
12	0,9845	-9,9262	-	-	-	-
13	0,9328	-34,5196	-	-	177	68
14	0,9736	-36,1221	-	-	191	42
15	0,9819	-20,6934	-	-	171	18,50
16	0,9614	-17,2417	-	-	126	47
17	0,9642	-11,3065	-	-	46	14,70
18	0,9899	-2,9952	-	-	281	56,50
19	0,9804	-11,6176	-	-	279	60,70
20	0,9652	-22,2235	-	-	130	29,40
21	0,9753	-22,4371	-	-	427	-25
22	0,9167	-29,4736	-	-	310	141
23	0,9491	-28,1209	-	-	424	90,60
24	0,9467	-30,7461	-	-	117	53,10
25	1,0024	-5,9132	-	-	-	-
26	0,9792	-19,9254	-	-	-	-
27	0,9846	-18,3020	-	-	368	59,60

28	0,9577	-25,9198	-	-	-	-
29	0,9966	-12,3997	-	-	174	-8
30	0,9816	-31,0205	-	-	-	-
31	0,9820	-24,1952	-	-	-	-
32	0,9918	-10,2699	-	-	-	-
33	1,0051	-1,3792	-	-	-	-
34	0,9648	-30,9167	-	-	125	39,80
35	0,9677	-29,6493	-	-	-	-
36	1,0042	-1,4491	-	-	-	-
37	0,9836	-35,5419	-	-	813	110
38	0,9943	-34,7636	-	-	612	-455
39	0,9744	-22,0506	-	-	404	135
40	0,9889	-27,0224	-	-	393	-111
41	0,9506	-16,5221	-	-	262	13,20
42	0,9689	-12,2606	-	-	229	183
43	0,9395	-16,3145	-	-	184	60,20
44	0,9410	-14,1448	-	-	139	53,70
45	0,9314	-34,2258	-	-	90,10	55,30

APPENDIX B - INTRODUCTION TO TAYLOR'S THEOREM FOR MULTIVARIABLE FUNCTIONS

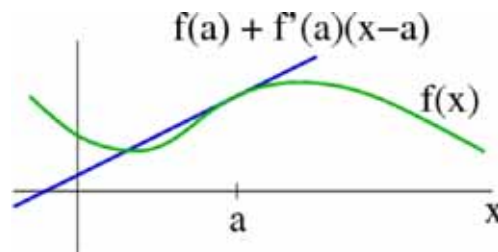
Source: http://mathinsight.org/taylors_theorem_multivariable_introduction

Remember one-variable calculus Taylor's theorem. Given a one variable function $f(x)$, you can fit it with a polynomial around $x=a$.

For example, the best linear approximation for $f(x)$ is

$$f(x) \approx f(a) + f'(a)(x-a).$$

This linear approximation fits $f(x)$ (shown in green below) with a line (shown in blue) through $x=a$ that matches the slope of f at a .



We can add additional, higher-order terms, to approximate $f(x)$ better near a . The best quadratic approximation is

$$f(x) \approx f(a) + f'(a)(x-a) + \frac{1}{2}f''(a)(x-a)^2$$

We could add third-order or even higher-order terms:

$$f(x) \approx f(a) + f'(a)(x-a) + \frac{1}{2}f''(a)(x-a)^2 + \frac{1}{6}f'''(a)(x-a)^3 + \dots$$

The important point is that this *Taylor polynomial* approximates $f(x)$ well for x near a . We want to generalize the Taylor polynomial to (scalar-valued) functions of multiple variables:

$$f(x) = f(x_1, x_2, \dots, x_n).$$

We already know the best linear approximation to f . It involves the derivative,

$$f(x) \approx f(a) + Df(a)(x-a).$$

where $Df(a)$ is the matrix of partial derivatives. The linear approximation is the first-order Taylor polynomial.

What about the second-order Taylor polynomial? To find a quadratic approximation, we need to add quadratic terms to our linear approximation. For a function of one-variable $f(x)$, the quadratic term was

$$\frac{1}{2} f''(a)(x-a)^2.$$

For a function of multiple variables $f(x)$, what is analogous to the second derivative?

Since $f(x)$ is scalar, the first derivative is $Df(x)$, a $1 \times n$ matrix, which we can view as an n -dimensional vector-valued function of the n -dimensional vector x . For the second derivative of $f(x)$, we can take the matrix of partial derivatives of the function $Df(x)$. We could write it as $DDf(x)$ for the moment. This second derivative matrix is an $n \times n$ matrix called the **Hessian matrix** of f . We'll denote it by $Hf(x)$,

$$Hf(x) = DDf(x).$$

When f is a function of multiple variables, the second derivative term in the Taylor series will use the Hessian $Hf(a)$. For the single-variable case, we could rewrite the quadratic expression as

$$\frac{1}{2} (x-a) f''(a) (x-a).$$

The analog of this expression for the multivariable case is

$$\frac{1}{2} (x-a)^T Hf(a) (x-a).$$

We can add the above expression to our first-order Taylor polynomial to obtain the second-order Taylor polynomial for functions of multiple variables:

$$f(x) \approx f(a) + Df(a)(x-a) + \frac{1}{2} (x-a)^T Hf(a)(x-a).$$

The second-order Taylor polynomial is a better approximation of $f(x)$ near $x=a$ than is the linear approximation (which is the same as the first-order Taylor polynomial). We'll be able to use it for things such as finding a local minimum or local maximum of the function $f(x)$.